

## Supporting Information

### **Through-Space Charge Transfer Delayed Fluorescence in Tris(triazolo)triazine Donor-Acceptor Copolymers**

Ryoga Hojo, Bruno T. Luppi, Katrina Bergmann, Zachary M. Hudson\*

*Department of Chemistry, The University of British Columbia, 2036 Main Mall, Vancouver, British Columbia, V6T 1Z1, Canada. E-mail: [zhudson@chem.ubc.ca](mailto:zhudson@chem.ubc.ca); Tel: +1-604-822-2691*

1.	General experimental details	S2-S4
2.	Synthetic procedures	S5-S8
3.	<sup>1</sup> H and <sup>13</sup> C{ <sup>1</sup> H} NMR spectra	S9-S15
4.	Differential scanning calorimetry and thermogravimetric analysis	S15-S16
5.	Photophysical properties	S16-S18
6.	Cyclic voltammetry and Tauc plots	S19
7.	Theoretical calculations	S20-S21
8.	Optimized structures of ground-state geometries	S21-S24
9.	Comparison to previously reported triazine based TSCT-TADF polymers	S25
10.	NMR tracking of the copolymerization	S26
11.	References	S27

## 1. General experimental details

**General considerations:** All reagents were purchased from Sigma-Aldrich, Oakwood Chemical, and Fischer Scientific and used without purification. Anhydrous and degassed solvents were obtained from Caledon Laboratories, dried using an Innovative Technologies Inc. solvent purification system. **TTT-3PhI**, *tert*-butyl prop-2-yn-1-ylcarbamate, **ACR-OH**, **NB-COOH** and Grubbs 3<sup>rd</sup> generation catalyst (G3, (IMesH<sub>2</sub>)(C<sub>5</sub>H<sub>5</sub>N)<sub>2</sub>(Cl)<sub>2</sub>Ru=CHPh) were synthesized according to previously reported procedures.<sup>1</sup> All yields correspond to the isolated yield. The <sup>1</sup>H and <sup>13</sup>C{<sup>1</sup>H} nuclear magnetic resonance (NMR) spectra were acquired using Bruker Advance 300 Spectrometer or Bruker AV III HD 400 MHz spectrometer with methylene chloride-*d*<sub>2</sub> (CD<sub>2</sub>Cl<sub>2</sub>), chloroform-*d* (CDCl<sub>3</sub>) or dimethylsulfoxide-*d*<sub>6</sub> (DMSO-*d*<sub>6</sub>) as the solvent. High-resolution mass spectra (HRMS) were obtained using the electrospray ionization (ESI) method. Absorbance measurements were taken using a Cary 60 spectrometer, while fluorescence measurements were obtained using an Edinburgh Instruments FLS1000 spectrofluorometer. Inert-atmosphere measurements were taken in an argon atmosphere for solid-state measurements, while for inert measurements in solution, the samples were prepared in an oxygen-free glove box and transferred to sealed cuvettes. Lifetimes ( $\tau_p$ ,  $\tau_d$ ) were analyzed via monoexponential tail-fitting. Absolute photoluminescence quantum yields were determined using an Edinburgh Instruments SC-30 Integrating Sphere Module.

**Size exclusion chromatography (SEC):** All measurements were conducted in chromatography-grade THF (flow rate = 1.0 mL min<sup>-1</sup>) at 35 °C using a Malvern OMNISEC system equipped with Viscotek TGuard guard column and Viscotek T600M and T3000 SEC columns. For the **poly(ACR)** homopolymer, the average molecular weight ( $M_n$  and  $M_w$ ) and polydispersity index ( $\mathbf{D}$ ) were obtained through absolute molecular weight determination using refractive index (RI), right-angle light scattering (RALS) and low-angle light scattering (LALS) detectors calibrated with a narrow 71 kDa polystyrene standard (Varian). For copolymers, differences in dn/dc between repeat units led to inaccurate results when using light scattering, therefore the molecular weights and  $\mathbf{D}$  were calculated by the conventional method relative to narrow-dispersity **poly(ACR)** homopolymers ( $\mathbf{D} \leq 1.1$ ) by creating a calibration curve ( $M_n = 32, 64, 270$  kDa) with the RI detector. Analyses were performed with the OMNISEC 11.36 (absolute calibration) or OMNISEC 4.6 (conventional calibration) software packages.

**Electrochemical and thermal characterization:** Cyclic voltammograms were acquired using a BASi Epsilon Eclipse potentiostat with a three-electrode configuration at ambient temperature. The three-electrode configuration consists of 3 mm diameter glassy carbon; a non-aqueous Ag/Ag<sup>+</sup> reference electrode in MeCN, which was referenced externally to ferrocene/ferrocenium (Fc<sup>0/+</sup>); and a counter electrode comprised of Pt wire. The electrolyte consisted of 0.2 M tetrabutylammonium hexafluorophosphate in 1,2-difluorobenzene. Experiments were conducted at a scan rate of 20 mV s<sup>-1</sup> in N<sub>2</sub>-sparged electrolyte solution with 2 mg mL<sup>-1</sup> of the analyte. For thermal characterization, thermogravimetric analysis (TGA) was performed using a TA Instruments TGA Q500 under N<sub>2</sub> flow (60 mL min<sup>-1</sup>) with a heating rate of 10 °C/min. Differential scanning calorimetry (DSC) was conducted under N<sub>2</sub> (50 mL min<sup>-1</sup>) using a NETZSCH DSC 214 Polyma instrument and a heating rate of 10 °C/min.

**Theoretical Calculations:** Quantum chemical calculations were conducted using the Gaussian 16 Rev. B.01 package unless otherwise stated.<sup>2</sup> Structures were optimized using density functional theory (DFT) at the M06-2X/def2-SVP level of theory to determine the ground state geometries.<sup>3,4</sup> Frequency analysis was performed at the same level of theory to verify the absence of imaginary frequencies.

The optimally tuned screened (OT-S) LC-PBE/def2-TZVP/IEFPCM(toluene) level of theory was used for all excited state calculations.<sup>4-6</sup> In range-separated (RS) functionals such as LC-PBE, a general expression for the separation of the exchange term into short- and long-range domains is defined by the interelectronic distance  $r$ .

$$\frac{1}{r} = \frac{\alpha + \beta \operatorname{erf}(\omega r)}{r} + \frac{1 - (\alpha + \beta \operatorname{erf}(\omega r))}{r} \quad (\text{S1})$$

In this expression,  $\alpha$ ,  $\beta$  and  $\omega$  are tunable parameters. By using Fock exchange for the first term on the right-hand side of equation S1 but semilocal exchange (such as the Perdew-Burke-Ernzerhof (PBE) functional)<sup>7</sup> for the second term, the exchange functional can be written as

$$E_X = \alpha E_F^{SR} + (1 - \alpha) E_{PBE}^S + (\alpha + \beta) E_F^{LR} + (1 - \alpha - \beta) E_{PBE}^{LR} \quad (\text{S2})$$

where subscripts ‘F’ and ‘PBE’ denote Fock and PBE exchange, and superscripts ‘SR’ and ‘LR’ denote short- and long-range, respectively. In this expression,  $\alpha$  determines the fraction of Fock exchange in the short-range,  $\alpha + \beta$  determines the fraction of Fock exchange in the long-range, and  $\omega$  is the range-separation parameter that determines the transition from short- to long-range.

To non-empirically tune all three parameters,  $\alpha$ ,  $\beta$  and  $\omega$  must fulfill Koopmans’ theorem, a fundamental property of exact Kohn-Sham theory that the exact functional must obey. This theorem equates the vertical ionization potential (IP) of an  $N$ -electron system to the negative of the highest occupied molecular orbital energy ( $\varepsilon_{HOMO}$ ). In donor-acceptor systems, it is also useful to include the electron affinity, which can be equated to the ionization potential of the anionic ( $N + 1$  electron) system.<sup>8</sup> Firstly,  $\omega$  is optimized in the gas phase with default values of  $\alpha$  and  $\beta$  where  $\alpha + \beta = 1$  to minimize the error measure  $J(\omega)$ :

$$J^2(\omega) = \sum_{i=0}^1 [\varepsilon_{HOMO}^{N+i}(\omega) + \text{IP}^{N+i}(\omega)]^2 \quad (\text{S3})$$

$$\text{IP}(N) = E_{GS}(N - 1) - E_{GS}(N) \quad (\text{S4})$$

For each  $\omega$  value tested, single point energy calculations were carried out on the  $N$ ,  $N - 1$  and  $N + 1$  electron systems in order to calculate  $J(\omega)$ , and minimization of  $J(\omega)$  was conducted using a golden section search. Possible  $\omega$  values for the minimization were limited between 0.0050 and 0.5000, with a tolerance criterion of 0.0010.

Once  $\omega$  was tuned in the gas phase, the polarizable continuum model (PCM) was invoked to tune  $\alpha$  and  $\beta$  such that  $\alpha + \beta = 1/\epsilon$  where  $\epsilon$  is the dielectric constant of the solvent used in the PCM.  $\alpha$  is tuned through minimization of  $J(\alpha)$ , and  $\beta$  is adjusted so the sum of  $\alpha$  and  $\beta$  remains fixed by the dielectric constant.

$$J^2(\alpha) = \sum_{i=0}^1 [\varepsilon_{HOMO}^{N+i}(\alpha) + \text{IP}^{N+i}(\alpha)]^2 \quad (\text{S5})$$

$J(\alpha)$  was minimized in an analogous method to  $J(\omega)$  but with the PCM present rather than in the gas phase. 2.3741 was used as the dielectric constant for toluene, and possible  $\alpha$  values for the minimization were limited between 0.0500 and 0.5000, with a tolerance criterion of 0.0010.

The parameters  $\alpha$ ,  $\beta$  and  $\omega$  were optimized individually for the ground state geometry of each molecule. At the ground state geometries, the first 50 singlet and triplet vertical excitations were analyzed using time-dependent DFT (TDDFT) under the Tamm-Dancoff approximation (TDA) at the (OT-S) LC-PBE/def2-TZVP/IEFPCM(toluene) level of theory using ORCA 5.0.3.<sup>9,10</sup>

Multiwfn 3.8 was used for non-covalent interaction (NCI) analysis and electron-hole analysis.<sup>11-13</sup> NCI analysis utilized wavefunction files from the M06-2X/def2-SVP optimization calculations, while electron-hole analysis utilized molden files from the (OT-S) LC-PBE/def2-TZVP/IEFPCM(toluene) TDDFT calculations.

VMD 1.9.3 was used to visualize the reduced density gradient (RDG) scatter plots, and RDG isosurfaces, with an isovalue of 0.63.<sup>14</sup> VESTA 3.5.7 was used to simultaneously visualize both the electron and hole isosurfaces, with an isovalue of 0.02.<sup>15</sup>

## 2. Synthetic procedures

**Synthesis of TTT-2PhI-Boc:** To a 500 mL Schlenk flask equipped with a magnetic stir bar was added **TTT-3PhI** (1.50 g, 1.86 mmol, 1.0 equiv.), Pd(PPh<sub>3</sub>)<sub>2</sub>Cl<sub>2</sub> (66 mg, 0.093 mmol, 0.05 equiv.), and CuI (35 mg, 0.186 mmol, 0.1 equiv.). The reaction vessel was placed under vacuum, then backfilled with N<sub>2</sub> gas three times. Next, anhydrous and oxygen-free THF (200 mL) was transferred into the vessel, followed by the addition of triethylamine (2.0 mL, 14.9 mmol, 8.0 equiv.) and tert-butyl prop-2-yn-1-ylcarbamate (290 mg, 1.86 mmol, 1.0 equiv.). The reaction was left to stir for 24 hours at room temperature. After the completion of the reaction as monitored by TLC, the reaction was quenched with 100 mL of saturated NH<sub>4</sub>Cl solution. The reaction mixture was then transferred to a 1 L round bottom flask, and THF was evaporated in vacuo. The aqueous layer was then extracted with EtOAc (50 mL x3), the combined organic phase was dried over MgSO<sub>4</sub>, and the crude mixture was concentrated in vacuo and purified over silica (1:4, EtOAc: Hexane). **TTT-2PhI-Boc:** Off-white solid. Yield: 420 mg (27%). <sup>1</sup>H NMR (400 MHz, DMSO-*d*<sub>6</sub>) δ 8.06 (d, *J* = 8.1 Hz, 4H), 8.02 (d, *J* = 8.1 Hz, 2H), 7.75 (d, *J* = 8.2 Hz, 4H), 7.55 (d, *J* = 8.1 Hz, 2H), 7.43 (s, 1H), 4.06 (d, *J* = 5.8 Hz, 2H), 1.42–3.32 (s, 9H) ppm. <sup>13</sup>C{<sup>1</sup>H} NMR (101 MHz, DMSO-*d*<sub>6</sub>) δ 155.3, 148.6, 148.6, 141.9, 137.5, 131.5, 131.4, 130.0, 125.5, 124.1, 123.9, 99.3, 90.4, 78.4, 30.2, 28.2 ppm: HRMS (FD) *m/z*: [M]<sup>+</sup> calc'd for [<sup>12</sup>C<sub>32</sub><sup>1</sup>H<sub>25</sub><sup>127</sup>I<sub>2</sub><sup>14</sup>N<sub>10</sub><sup>16</sup>O<sub>2</sub>]<sup>+</sup> 835.02848; difference 4.01 ppm.

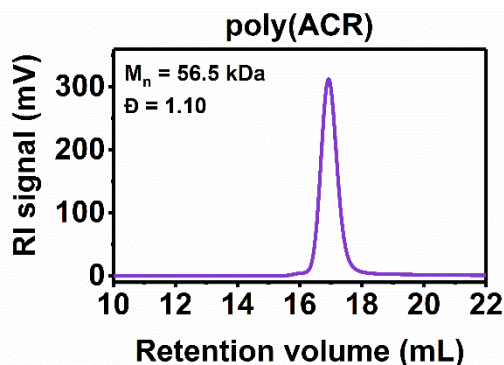
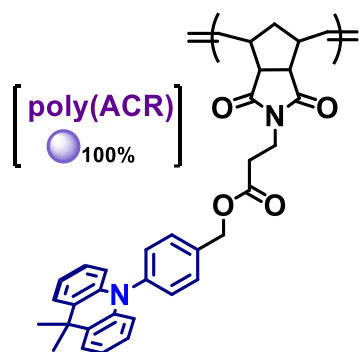
**Synthesis of TTT-2Oct-Boc:** To a 250 mL Schlenk flask equipped with a magnetic stir bar was added **TTT-2PhI-Boc** (520 mg, 0.623 mmol, 1.0 equiv.), Pd(PPh<sub>3</sub>)<sub>2</sub>Cl<sub>2</sub> (31 mg, 0.044 mmol, 0.07 equiv.), and CuI (20 mg, 0.93 mmol, 0.15 equiv.). The reaction vessel was placed under vacuum, then backfilled with N<sub>2</sub> gas three times. Next, anhydrous and oxygen-free THF (125 mL) was transferred into the vessel, followed by the addition of triethylamine (0.95 mL, 6.86 mmol, 11. equiv.) and 1-octyne (1.00 mL, 6.86 mmol, 11. equiv.). The reaction was left to stir for 48 hours at room temperature. After the completion of the reaction monitored by TLC, the reaction was quenched with 50 mL of saturated NH<sub>4</sub>Cl solution. The reaction mixture was transferred to a 250 mL round bottom flask, and THF was evaporated using rotary evaporation. The aqueous layer was then extracted with EtOAc (50 mL x3), the combined organic phase was dried over MgSO<sub>4</sub>, and the crude mixture was concentrated in vacuo and purified over silica (1:4, EtOAc: Hexane). **TTT-2Oct-Boc:** Off-white solid. Yield: 426 mg (87%). <sup>1</sup>H NMR (400 MHz, CD<sub>2</sub>Cl<sub>2</sub>-*d*<sub>2</sub>) δ 8.05–8.01 (m, 6H), 7.61–7.56 (m, 6H), 5.03 (s, 1H), 4.16 (d, *J* = 5.8 Hz, 2H), 2.48 (t, *J* = 7.1 Hz, 4H), 1.66 (qu, *J* = 7.1 Hz, 4H), 1.53–1.27 (m, 21H), 0.93 (t, *J* = 6.3 Hz, 6H) ppm. <sup>13</sup>C{<sup>1</sup>H} NMR (101 MHz, CD<sub>2</sub>Cl<sub>2</sub>-*d*<sub>2</sub>): δ 155.6, 150.7, 150.5, 141.2, 141.1, 132.0, 131.8, 130.4, 130.3, 128.4, 126.8, 124.1, 123.2, 123.1, 94.5, 89.3, 82.2, 80.2, 31.8, 29.0, 29.0, 28.5, 23.0, 19.9, 14.3 ppm: HRMS (FD) *m/z*: [M]<sup>+</sup> calc'd for [<sup>12</sup>C<sub>48</sub><sup>1</sup>H<sub>52</sub><sup>14</sup>N<sub>10</sub><sup>16</sup>O<sub>2</sub>]<sup>+</sup> 800.43145; difference 4.97 ppm.

**Synthesis of TTT-2Oct-NH<sub>2</sub>:** **TTT-2Oct-Boc** (380 mg, 0.455 mmol, 1.0 equiv.) was transferred to a 20 mL vial equipped with a magnetic stir-bar, followed by the addition of 1,4-dioxane (5 mL) and 4M HCl (5 mL). The reaction was left to stir under air at room temperature for 1 hour. After the completion of the reaction as monitored by TLC, 10 mL of distilled water and 20 mL of diethyl ether were added to separate the solution into organic and aqueous phases. The organic phase was then separated via a separatory funnel, and the aqueous phase was extracted with EtOAc (20 mL

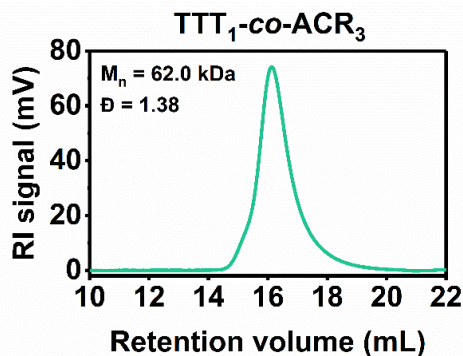
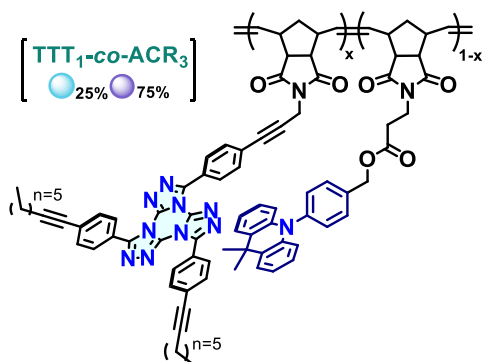
x 3). Finally, the combined organic phase was dried over MgSO<sub>4</sub>, and the crude mixture was concentrated in vacuo. **TTT-2Oct-NH<sub>2</sub>**: Crystalline and brown solid. Yield: 322 mg (90%). <sup>1</sup>H NMR (400 MHz, DMSO-*d*<sub>6</sub>) δ 8.08 (d, *J* = 8.0 Hz, 2H), 7.99 (d, *J* = 8.0 Hz, 4H), 7.75 (d, *J* = 8.0 Hz, 2H), 7.66 (d, *J* = 8.0 Hz, 2H), 4.02 (s, 2H), 2.52-2.48 (m, 4H), 1.59 (q, *J* = 7.0 Hz, 4H), 1.47 (sept, *J* = 6.4 Hz, 4H), 1.44-1.24 (m, 8H) 0.88 (t, *J* = 6.3 Hz, 6H) ppm. <sup>13</sup>C{<sup>1</sup>H} NMR (101 MHz, DMSO-*d*<sub>6</sub>) δ 148.7, 148.5, 142.0, 141.9, 131.5, 131.3, 130.2, 130.0, 126.4, 124.9, 124.4, 123.6, 93.8, 80.0, 30.8, 28.0, 28.0, 22.0, 18.7, 14.0 ppm. Note: the molecular ion for TTT-2Oct-Boc could not be detected by HRMS in either ESI or FD modes. The product was however carried through the synthesis to give **TTT-NB**, which was successfully characterized by HRMS.

**Synthesis of TTT-NB:** To a 100 mL round bottom flask equipped with a magnetic stir bar was added **TTT-2Oct-NH<sub>2</sub>** (291 mg, 0.416 mmol, 1.0 equiv.) and cis-5-norbornene-exo-2,3-dicarboxylic anhydride (82 mg, 0.50 mmol, 1.2 equiv.). Next, 50 mL of toluene was added to the vessel, followed by a catalytic amount of triethylamine (0.02 mL, 0.125 mmol, 0.30 equiv.). A Dean-Stark trap was then attached to the reaction vessel before the reaction was heated to reflux at 120 °C for 18 hours. After the completion of the reaction as monitored by TLC, the toluene solution was evaporated in vacuo before being redissolved in 50 mL of EtOAc, dried over MgSO<sub>4</sub>, and the crude mixture was concentrated in vacuo. The concentrated solution with the product was purified over silica (1:9, EtOAc: Hexane). **TTT-NB**: brown solid. Yield: 221 mg (63%). <sup>1</sup>H NMR (400 MHz, CD<sub>2</sub>Cl<sub>2</sub>-*d*<sub>2</sub>) δ 8.10-8.05 (m, 6H) 7.64-7.60 (m, 6H), 6.33 (s, 2H), 4.48 (s, 2H), 3.31 (s, 2H), 2.76 (s, 2H), 2.48 (t, *J* = 7.1 Hz, 4H) 1.68-1.63 (m, 5H), 1.56-1.45 (m, 6H), 1.38-1.26 (m, 10H), 0.95-0.90 (m, 6H) ppm. <sup>13</sup>C{<sup>1</sup>H} NMR (101 MHz, CD<sub>2</sub>Cl<sub>2</sub>-*d*<sub>2</sub>) δ 177.0, 150.7, 150.5, 141.2, 141.1, 138.3, 132.2, 131.8, 130.4, 130.4, 128.4, 126.3, 124.3, 123.2, 94.5, 85.7, 82.0, 80.1, 48.3, 46.0, 43.1, 31.8, 29.0, 29.0, 28.7, 23.0, 19.9, 14.3 ppm: HRMS (FD) *m/z*: [M]<sup>+</sup> calc'd for [C<sub>52</sub>H<sub>48</sub>N<sub>10</sub>O<sub>2</sub>]<sup>+</sup> 844.42; difference 2.00 ppm.

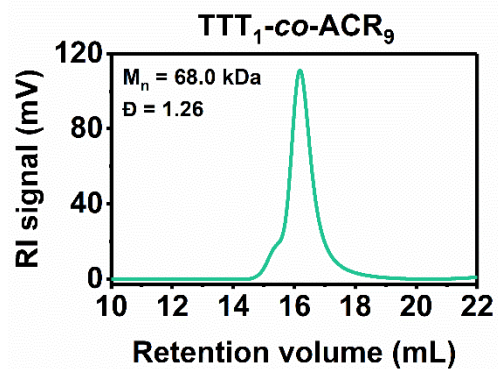
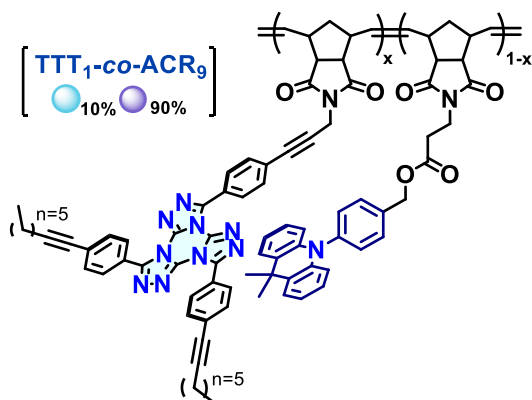
**Synthesis of ACR-NB:** To a 250 mL Schlenk flask equipped with a magnetic stir bar was added ACR-OH (550 mg, 1.74 mmol, 1.0 equiv.), NB-COOH (615 mg, 2.62 mol, 1.50 equiv.), and 4-dimethylaminopyridine (DMAP) (15 mg, 0.133 mmol, 0.065 equiv.). Anhydrous CH<sub>2</sub>Cl<sub>2</sub> was then added and the mixture cooled to 0 °C before *N,N'*-dicyclohexylcarbodiimide (DCC) (432 mg, 2.09 mmol, 1.2 equiv.) was added. The reaction mixture was allowed to warm up to room temperature and left to stir for 24 hours. After the completion of the reaction as monitored by TLC, the reaction mixture was filtered to remove precipitates of 1,3-dicyclohexyl urea, and the filtrate was dried over MgSO<sub>4</sub>, and the crude mixture was concentrated in vacuo. The concentrated solution with the product was purified over silica (1:4, EtOAc: Hexane). **ACR-NB**: White solid. Yield: 623 mg (67%). <sup>1</sup>H NMR (400 MHz, CD<sub>2</sub>Cl<sub>2</sub>-*d*<sub>2</sub>) δ 7.62 (dd, *J* = 1.6, 2.2 Hz, 2H), 7.45 (dd, *J* = 1.6, 2.2 Hz, 2H), 7.33 (dd, *J* = 1.6, 2.2 Hz, 2H), 6.97-6.89 (m, 4H), 6.28 (t, *J* = 1.9 Hz, 2H), 6.24 (dd, *J* = 5.9, 1.6 Hz, 2H), 5.22 (s, 2H), 3.81 (t, *J* = 7.2 Hz, 2H), 3.23-3.21 (m, 2H), 2.71 (t, *J* = 7.1 Hz, 2H), 2.66 (s, 2H), 1.67 (s, 6H), 1.45 (dd, *J* = 8.3, 1.6 Hz, 1H), 1.26 (dd, *J* = 8.4, 1.6 Hz, 1H) ppm. <sup>13</sup>C{<sup>1</sup>H} NMR (101 MHz, CD<sub>2</sub>Cl<sub>2</sub>-*d*<sub>2</sub>) δ 177.9, 171.0, 141.6, 141.2, 138.2, 136.4, 131.8, 131.1, 130.5, 126.7, 125.6, 120.9, 114.4, 66.5, 48.2, 45.7, 43.1, 36.3, 34.8, 32.6, 31.4 ppm: HRMS (FD) *m/z*: [M]<sup>+</sup> calc'd for [<sup>12</sup>C<sub>34</sub><sup>1</sup>H<sub>32</sub><sup>14</sup>N<sub>2</sub><sup>16</sup>O<sub>4</sub>]<sup>+</sup> 532.23621; difference -1.64 ppm.



**Synthesis of poly(ACR):** Under an  $N_2$  atmosphere, a solution of **ACR-NB** (99.2 mg, 0.186 mmol) was prepared in 7.45 mL of  $CH_2Cl_2$ . To this mixture, 165  $\mu L$  of a solution of Grubbs' 3rd generation catalyst in  $CH_2Cl_2$  (0.011 M, 0.00182 mmol) was added in one portion with stirring. After 3 h, NMR indicated completion of the polymerization through disappearance of the monomer's vinylic proton signals, so the polymerization was quenched by addition of 0.5 mL of ethyl vinyl ether. The mixture was stirred for an additional 5 minutes, then precipitated into 50 mL of MeOH under air. The supernatant was decanted, and the precipitate was purified by preparatory SEC in THF, followed by another precipitation in 50 mL of MeOH, filtration, and drying under vacuum at 60 °C to afford **poly(ACR)** as a white solid (63.9 mg, 64 %).  $M_n = 56.5$  kDa (absolute),  $\text{Đ} = 1.10$ .  $T_g = 138$  °C.



**Synthesis of  $TTT_1-co-ACR_3$ :** Under  $N_2$  atmosphere, a solution of **ACR-NB** (51.1 mg, 0.0949 mmol) and **TTT-NB** (27.0 mg, 0.0320 mmol) was prepared in 5.12 mL of  $CH_2Cl_2$ . To this mixture, 113  $\mu L$  of a solution of Grubbs' 3rd generation catalyst in  $CH_2Cl_2$  (0.011 M, 0.00124 mmol) was added in one portion under stirring. After 3 h, NMR indicated completion of the polymerization through the disappearance of the monomers' vinylic proton signals, so the polymerization was quenched by addition of 0.5 mL of ethyl vinyl ether. The mixture was stirred for an additional 5 minutes, then precipitated into 50 mL of MeOH under air. The supernatant was decanted, and the precipitate was purified by preparatory SEC in THF, followed by another precipitation in 50 mL of MeOH, filtration, and drying under vacuum at 60 °C to afford  **$TTT_1-co-ACR_3$**  as a beige solid (53.4 mg, 68 %).  $M_n = 62$  kDa (relative to **poly(ACR)** standards),  $\text{Đ} = 1.38$ .  $T_g = 140$  °C.



**Synthesis of  $\text{TTT}_1\text{-co-ACR}_9$ :** Under  $\text{N}_2$  atmosphere, a solution of **ACR-NB** (70.0 mg, 0.131 mmol) and **TTT-NB** (12.3 mg, 0.0146 mmol) was prepared in 5.84 mL of  $\text{CH}_2\text{Cl}_2$ . To this mixture, 129  $\mu\text{L}$  of a solution of Grubbs' 3rd generation catalyst in  $\text{CH}_2\text{Cl}_2$  (0.011 M, 0.00142 mmol) was added in one portion under stirring. After 3 h, NMR indicated completion of the polymerization through disappearance of the monomers' vinylic H signals, so the polymerization was quenched by addition of 0.5 mL of ethyl vinyl ether. The mixture was stirred for an additional 5 minutes, then precipitated over 50 mL of MeOH under air. The supernatant was decanted, and the precipitate was purified by preparatory SEC in THF, followed by another precipitation in 50 mL of MeOH, filtration, and drying under vacuum at 60  $^\circ\text{C}$  to afford  **$\text{TTT}_1\text{-co-ACR}_3$**  as a beige solid (52.8 mg, 64 %).  $M_n = 68.0$  kDa (relative to **poly(ACR)**),  $\bar{D} = 1.26$ .  $T_g = 143$   $^\circ\text{C}$ .



3.  $^1\text{H}$  and  $^{13}\text{C}\{^1\text{H}\}$  NMR spectra

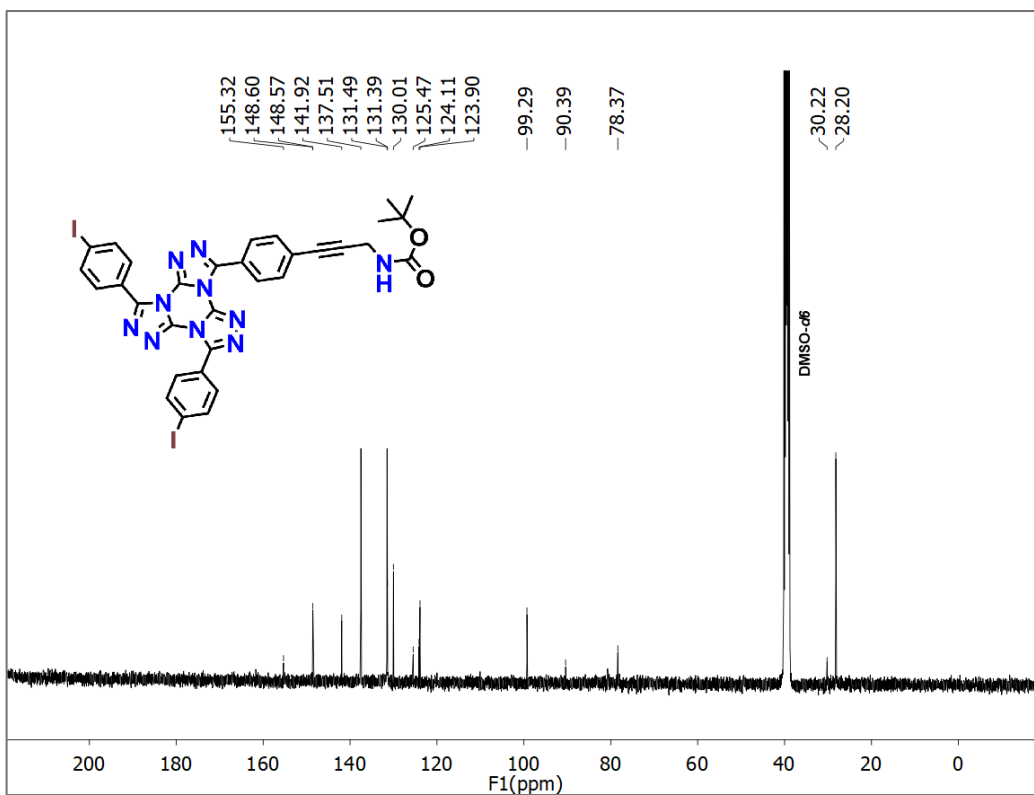
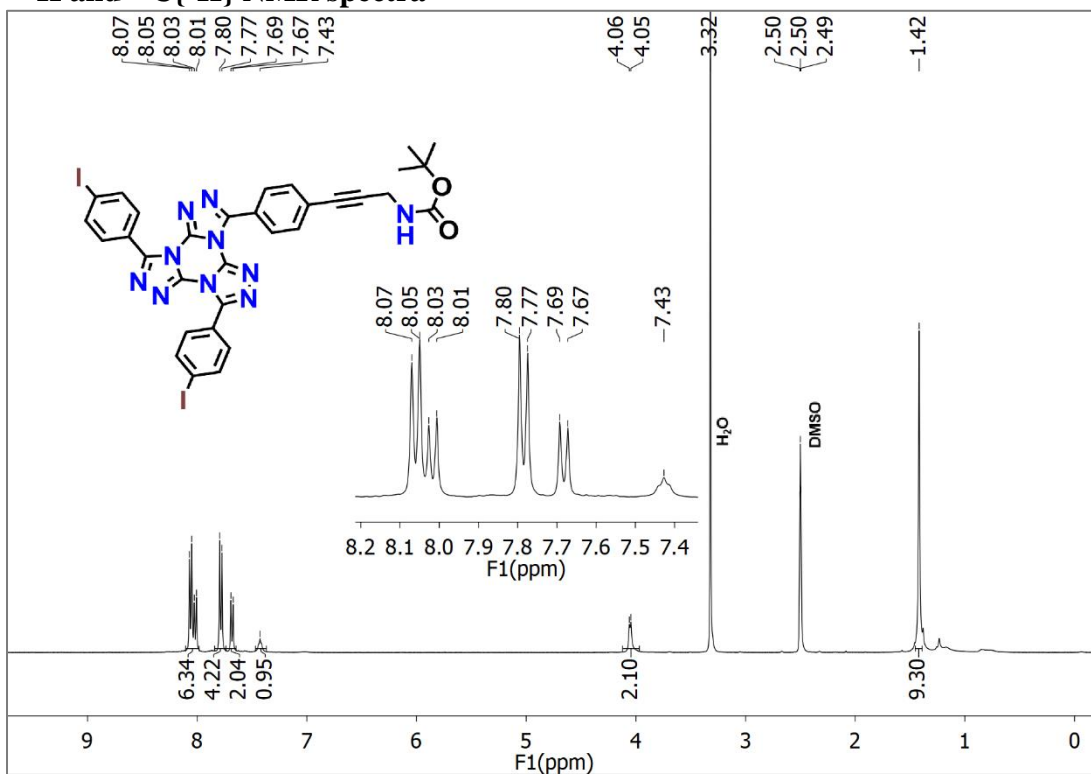


**Figure S2.  $^{13}\text{C}\{^1\text{H}\}$ -NMR spectrum of TTT-2PhI-Boc (DMSO- $d_6$ , 400 MHz).**

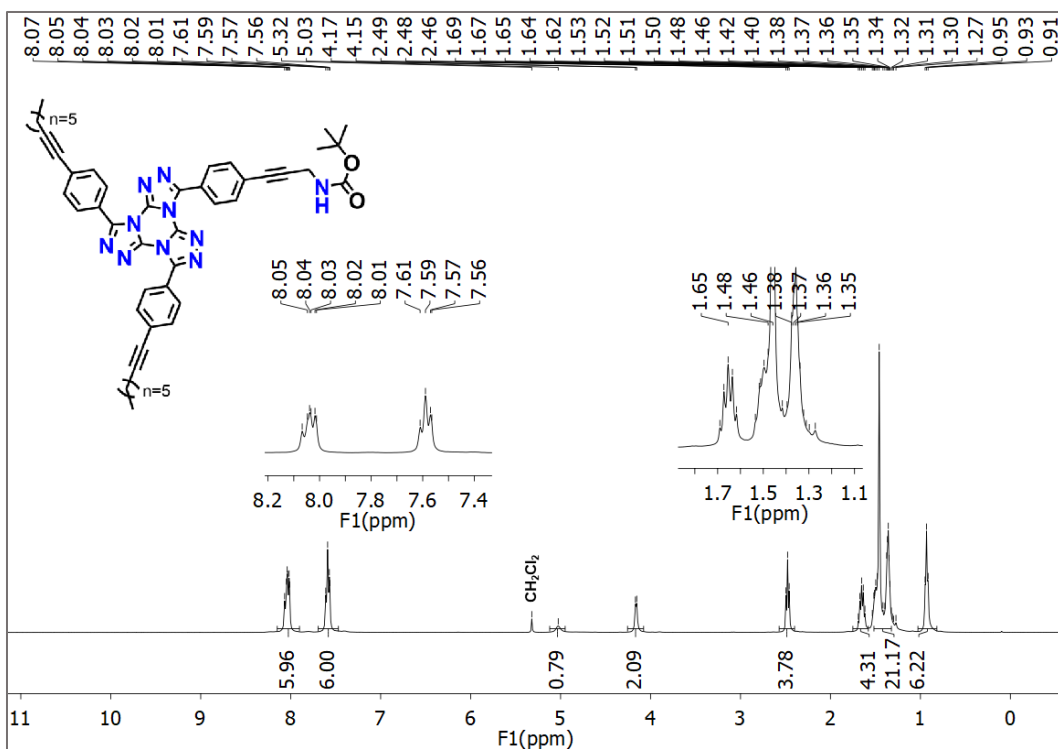


Figure S3. <sup>1</sup>H-NMR spectrum of TTT-2Oct-Boc (CD<sub>2</sub>Cl<sub>2</sub>-d<sub>2</sub>, 400 MHz).

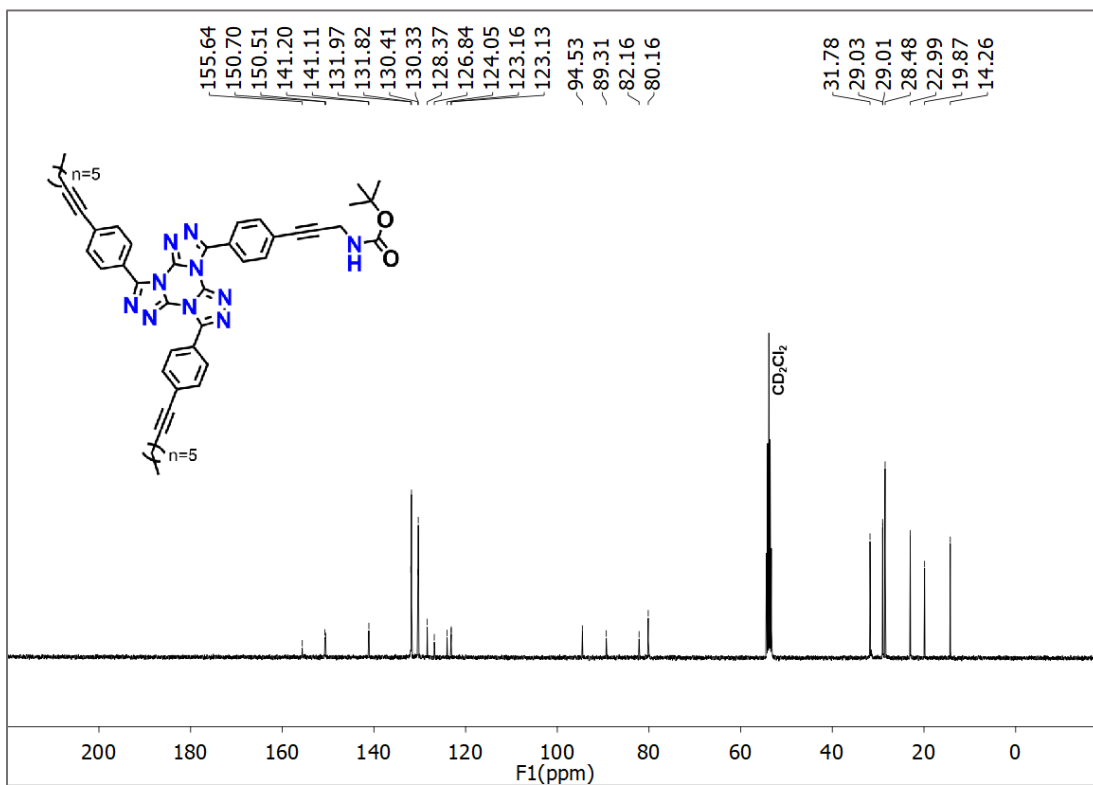
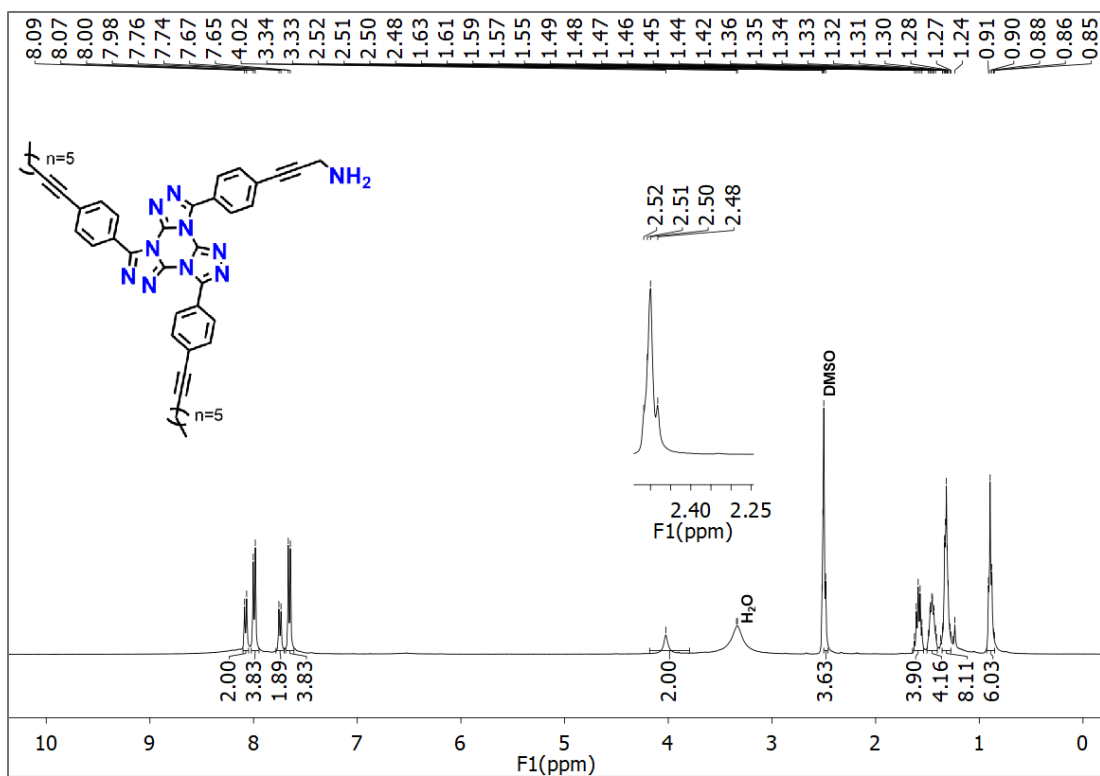
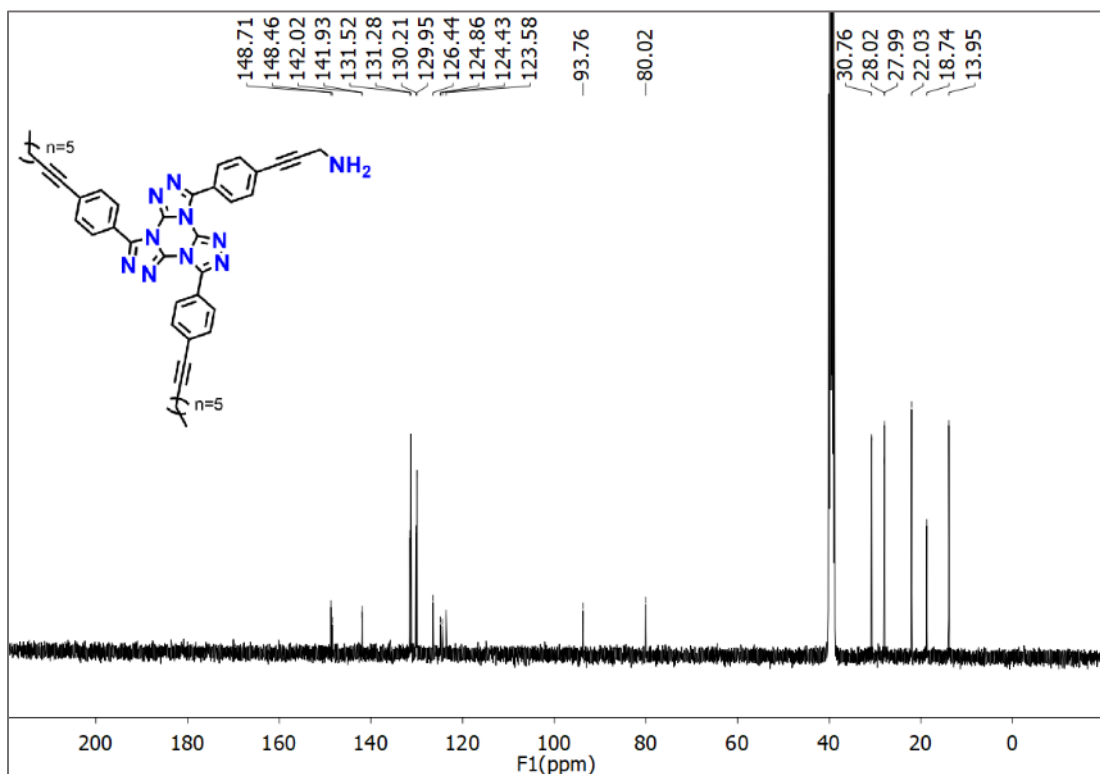


Figure S4. <sup>13</sup>C{<sup>1</sup>H}-NMR spectrum of TTT-2Oct-Boc (CD<sub>2</sub>Cl<sub>2</sub>-d<sub>2</sub>, 400 MHz).



**Figure S5.** <sup>1</sup>H-NMR spectrum of TTT-2Oct-NH<sub>2</sub> (DMSO-*d*<sub>6</sub>, 400 MHz).



**Figure S6.** <sup>13</sup>C{<sup>1</sup>H}-NMR spectrum of TTT-2Oct-NH<sub>2</sub> (DMSO-*d*<sub>6</sub>, 400 MHz).

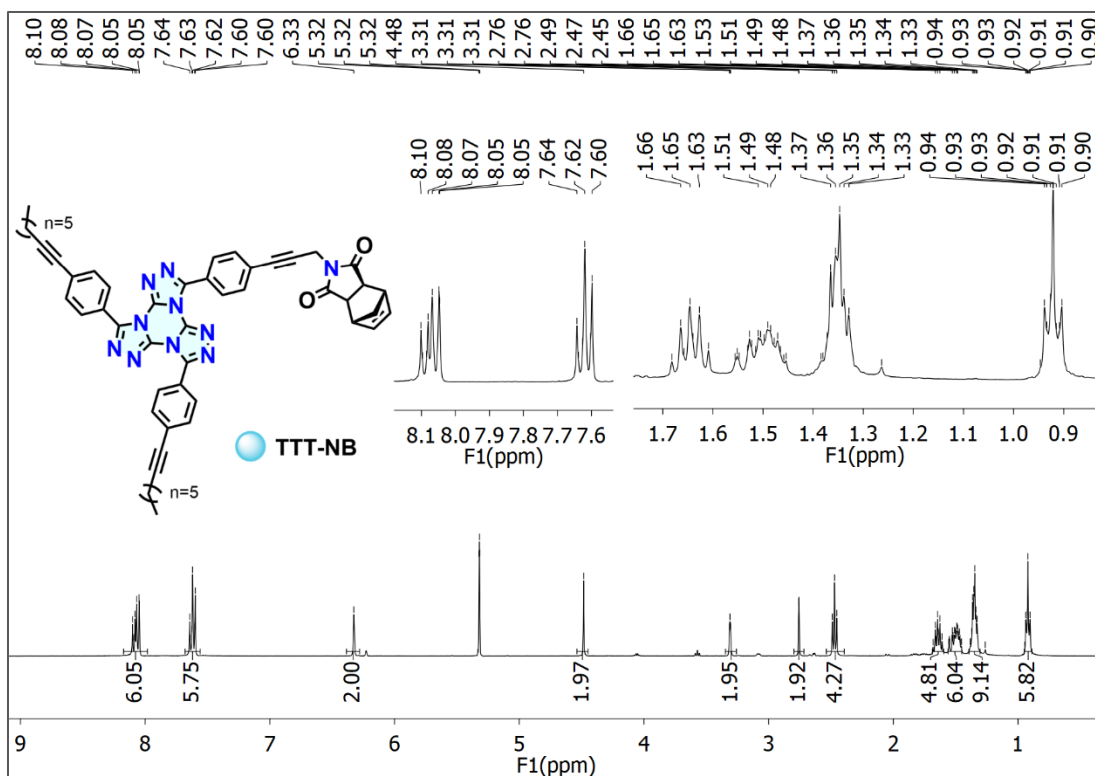


**Figure S7.**  $^1\text{H-NMR}$  spectrum of **TTT-NB** ( $\text{CD}_2\text{Cl}_2-d_2$ , 400 MHz).

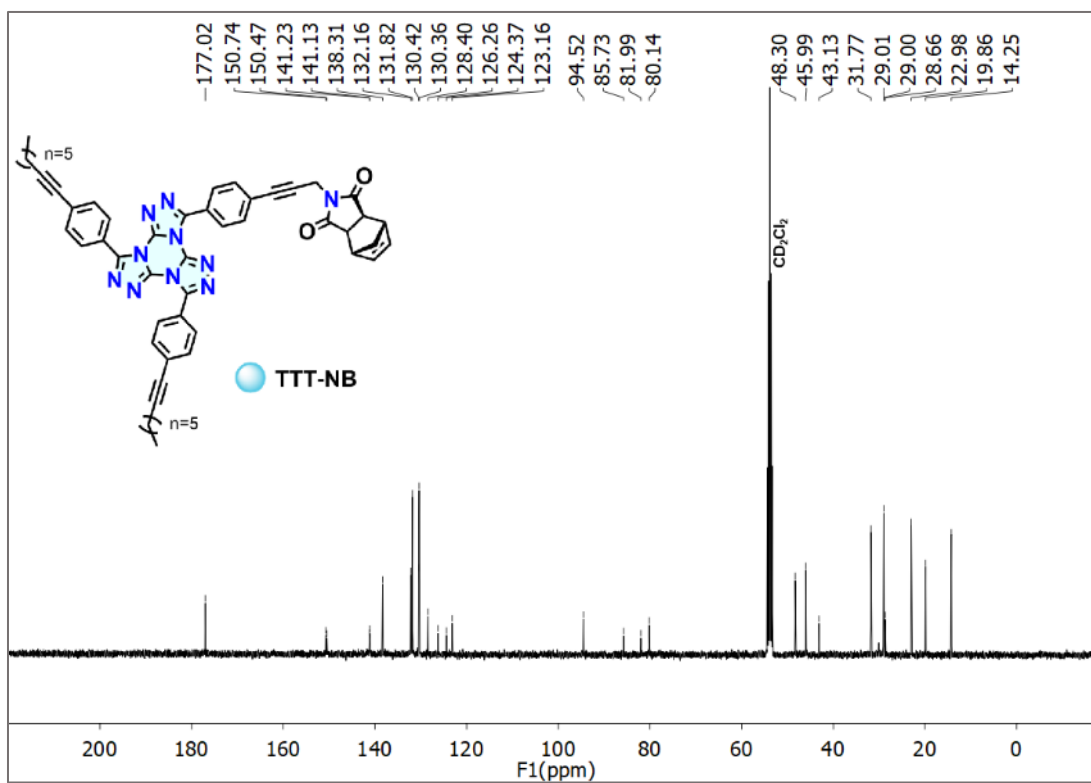


**Figure S8.**  $^{13}\text{C}\{^1\text{H}\}$ -NMR spectrum of **TTT-NB** ( $\text{CD}_2\text{Cl}_2-d_2$ , 400 MHz).

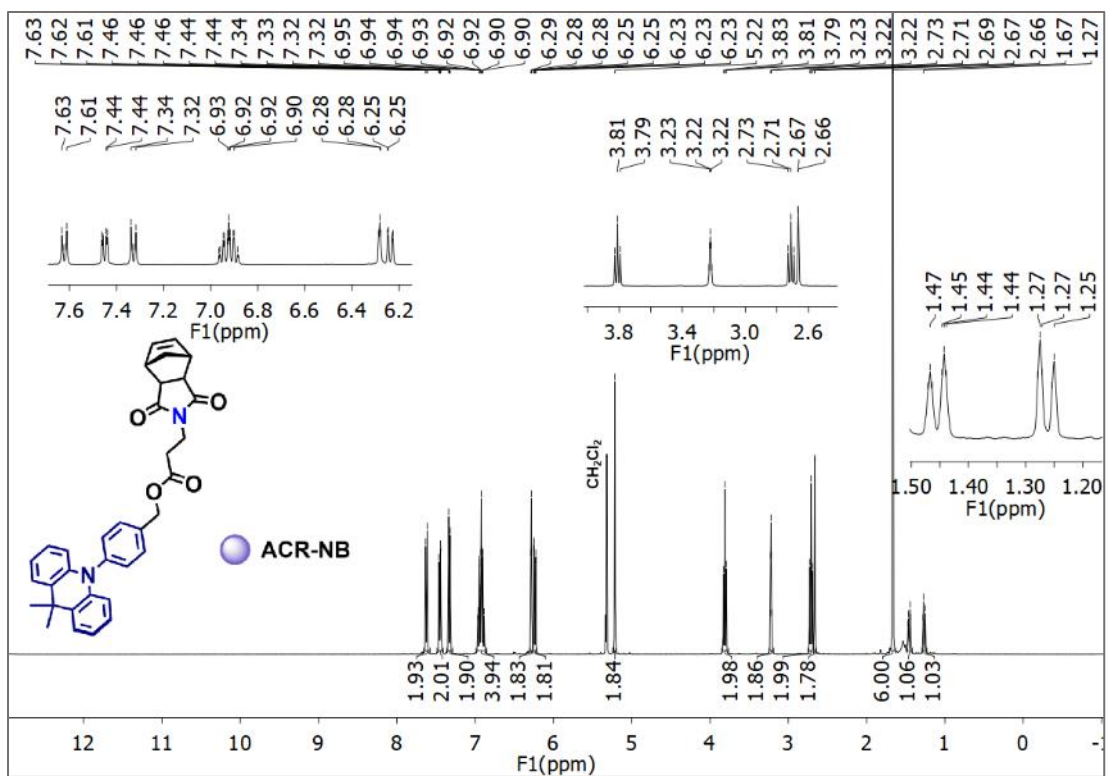


**Figure S9.**  $^1\text{H}$ -NMR spectrum of ACR-NB ( $\text{CD}_2\text{Cl}_2$ - $d_2$ , 400 MHz).

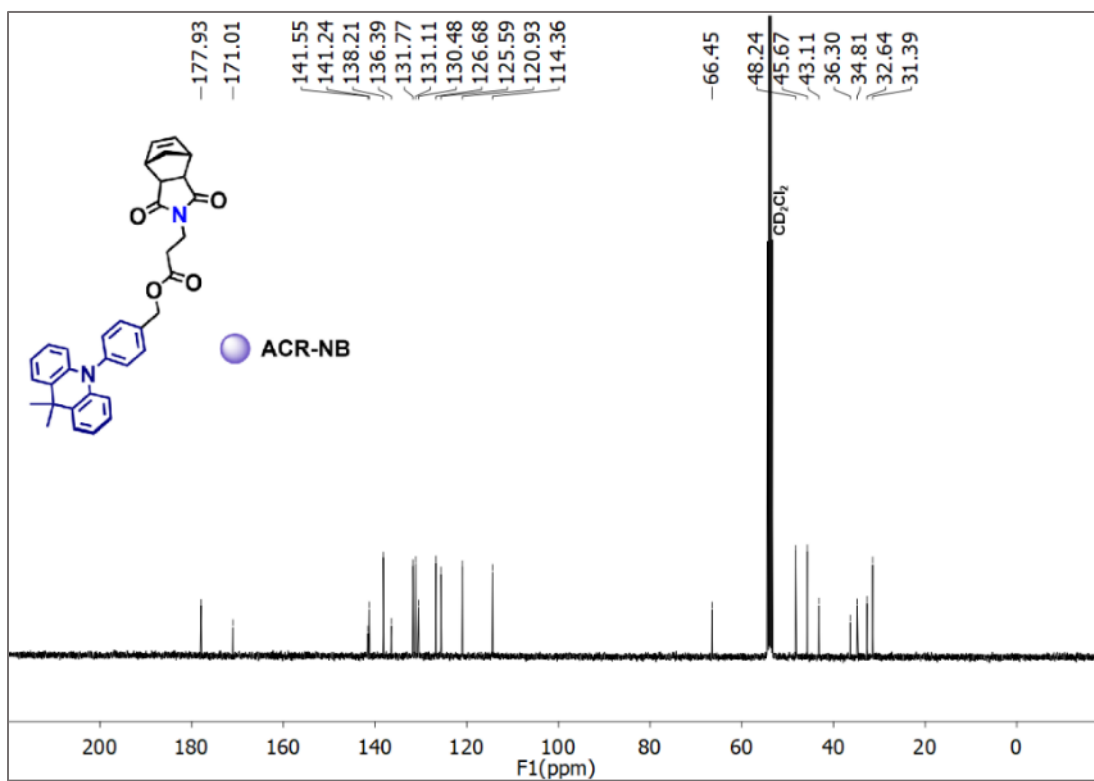


**Figure S10.**  $^{13}\text{C}\{^1\text{H}\}$ -NMR spectrum of ACR-NB ( $\text{CD}_2\text{Cl}_2$ - $d_2$ , 400 MHz).

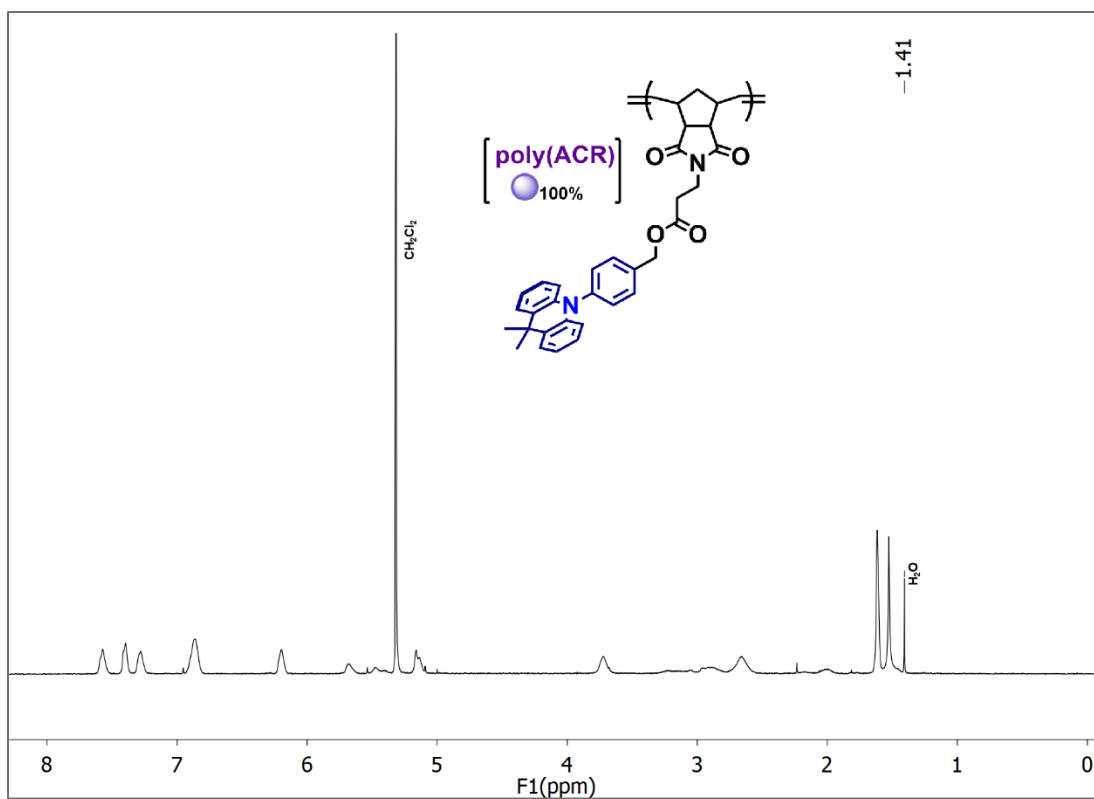


**Figure S11.**  $^1\text{H-NMR}$  spectrum of **poly(ACR)** ( $\text{CD}_2\text{Cl}_2-d_2$ , 400 MHz).

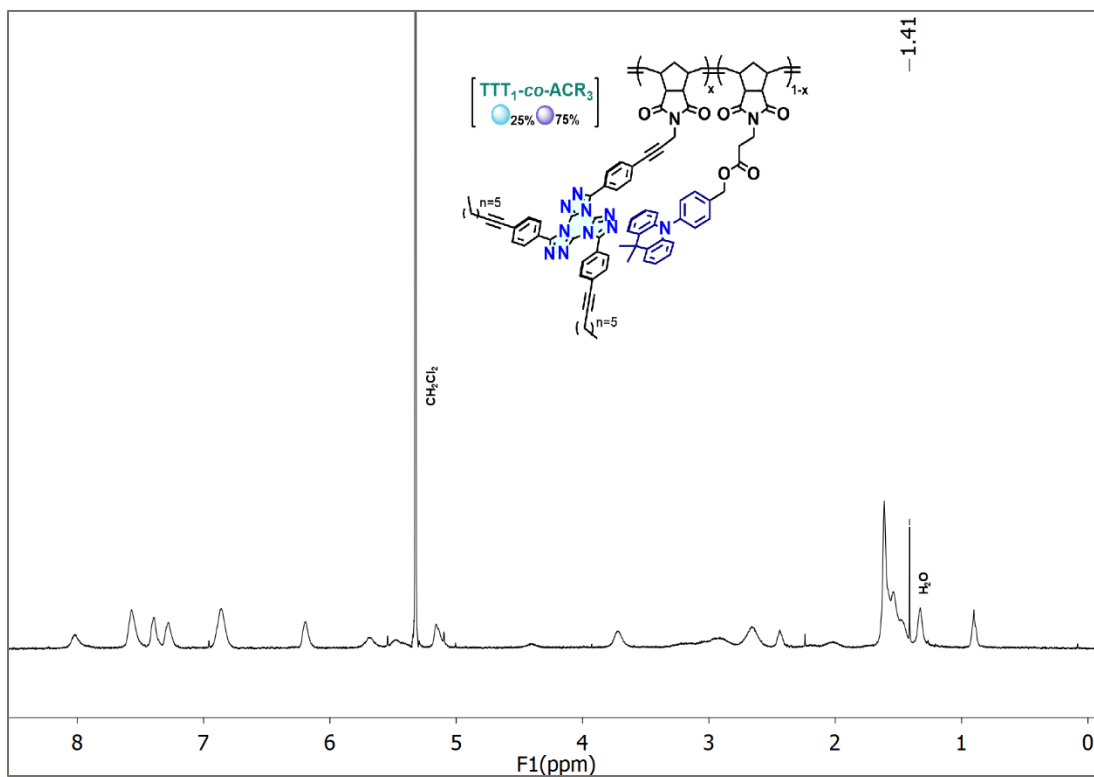


**Figure S12.**  $^1\text{H-NMR}$  spectrum of **TTT<sub>1</sub>-co-ACR<sub>3</sub>** ( $\text{CD}_2\text{Cl}_2-d_2$ , 400 MHz).

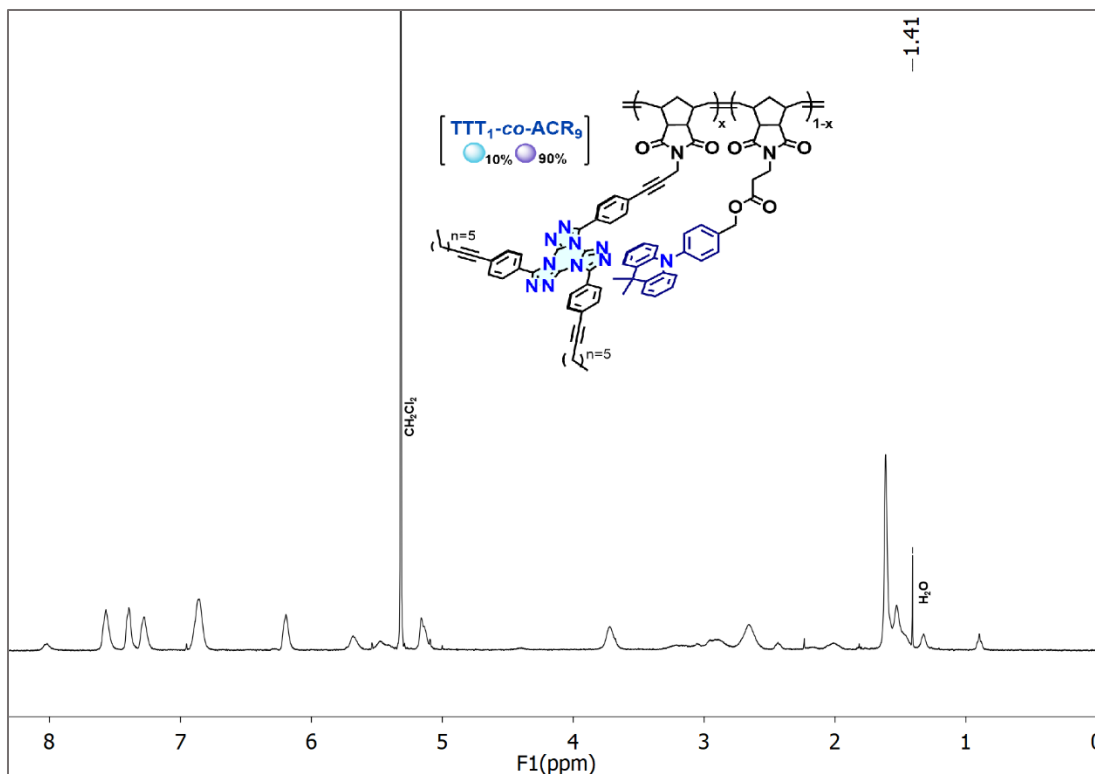


**Figure S13.**  $^1\text{H-NMR}$  spectrum of  $\text{TTT}_1\text{-co-ACR}_9$  ( $\text{CD}_2\text{Cl}_2\text{-}d_2$ , 400 MHz).

#### 4. DSC/TGA

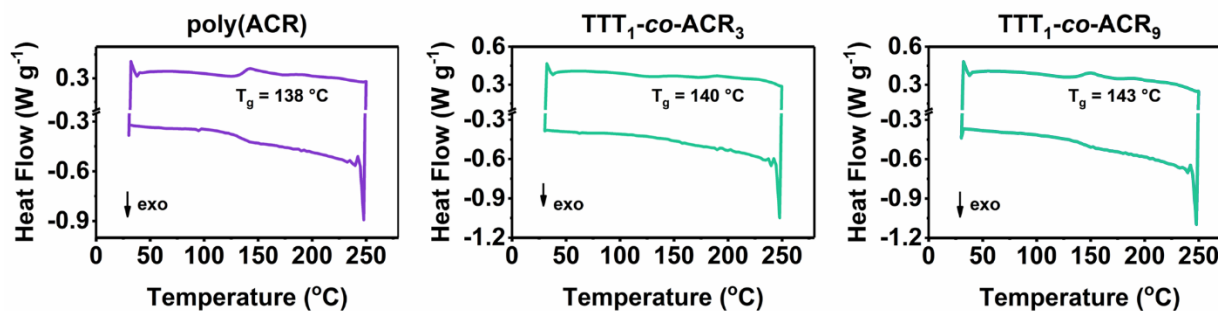


**Figure S14.** DSC traces of polymers at a rate of  $10\text{ }^\circ\text{C min}^{-1}$ , under a  $50\text{ mL min}^{-1}$  flow of nitrogen gas. The plotted traces correspond to the second heating cycle.

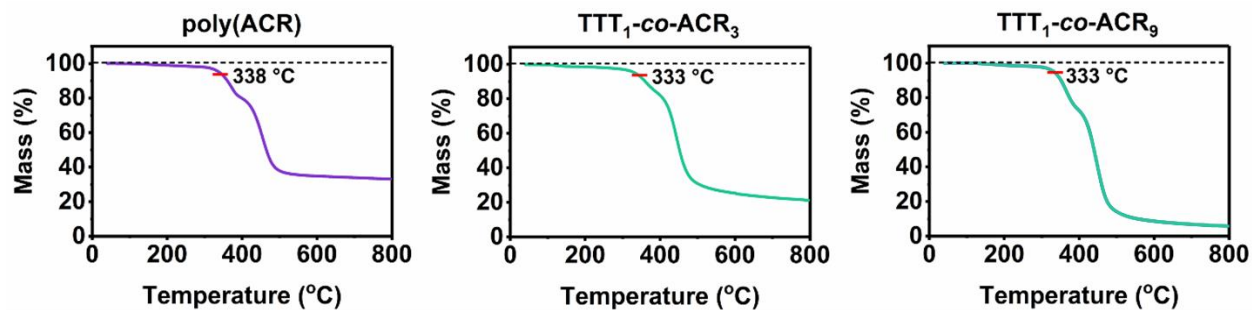


**Figure S15.** TGA performed for polymers at a rate of 10 °C min<sup>-1</sup>, under a 50 mL min<sup>-1</sup> flow of nitrogen gas, with temperature at 5% weight loss indicated.

## 5. Photophysical properties

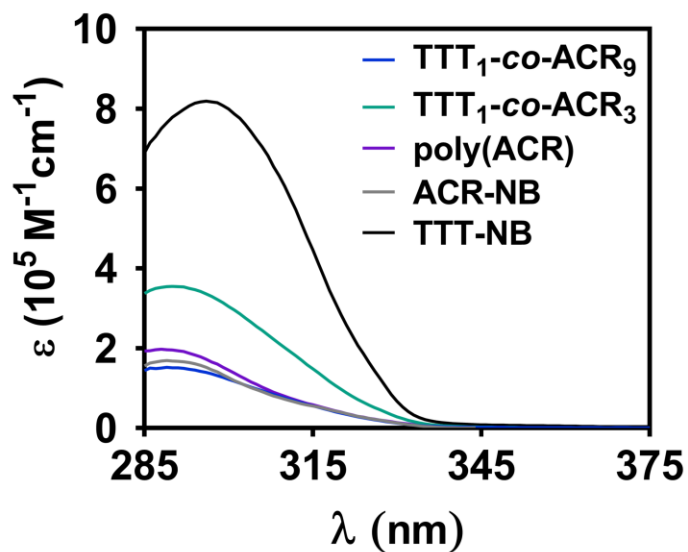


**Figure S16.** UV-Vis spectra of all materials in toluene (concentration = 0.01 mg mL<sup>-1</sup>).



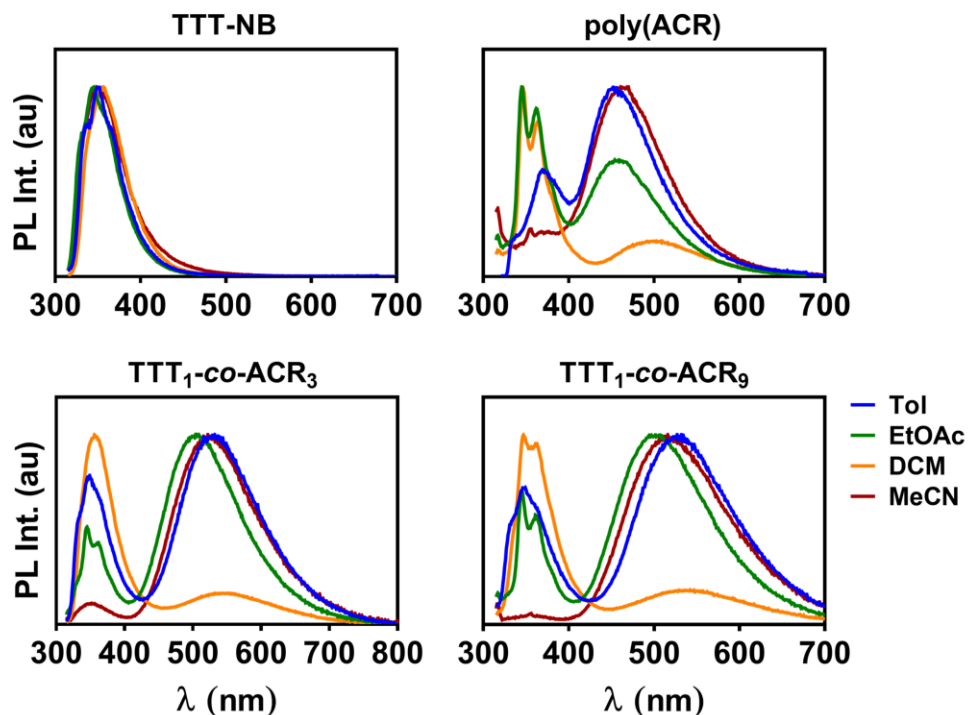


**Figure S17.** Solvatochromism experiments of the polymers in addition to **TTT-NB** (Concentration = 0.01 mg/mL, ex = 290 nm). For **TTT<sub>1</sub>-co-ACR<sub>3</sub>** and **TTT<sub>1</sub>-co-ACR<sub>9</sub>**, the spectra are zoomed in from 400 to 800 nm and normalized to highlight TSCT emission.

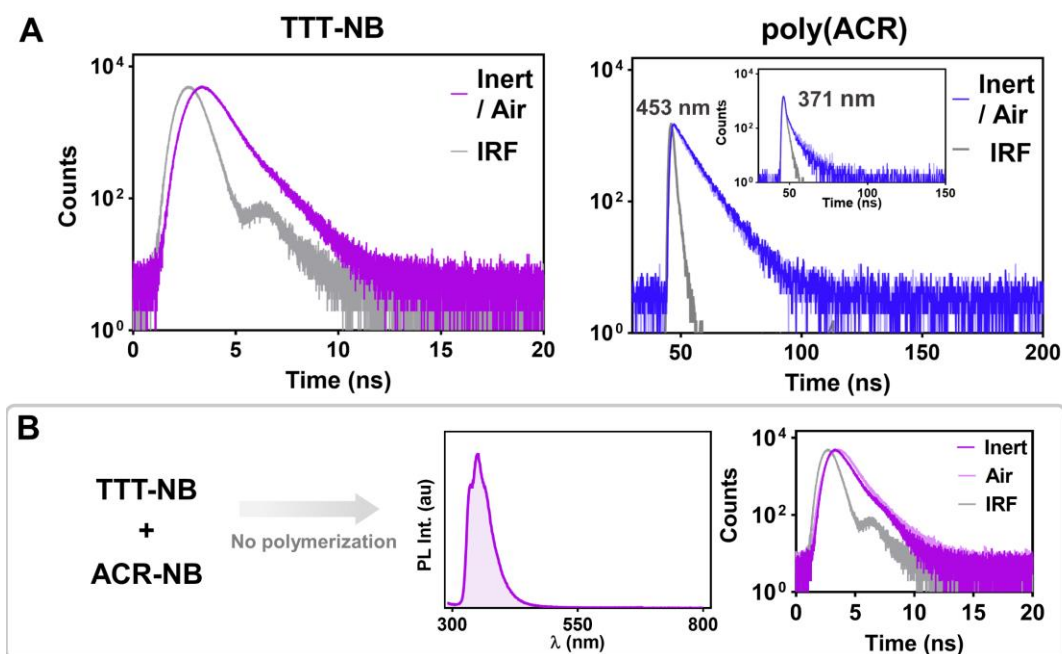


**Figure S18.** (A) Inert vs air conditions for prompt PL decays of **TTT-NB** and **poly(ACR)** in toluene (measured using TCSPC, concentration: 0.01 mg mL<sup>-1</sup>, ex = 313 nm). (B) control experiments showing emission and prompt PL decay of 1:3 molar ratio of **TTT-NB** and **ACR-NB** in toluene (measured using TCSPC, total concentration of monomers = 0.01 mg mL<sup>-1</sup>, ex = 313 nm).

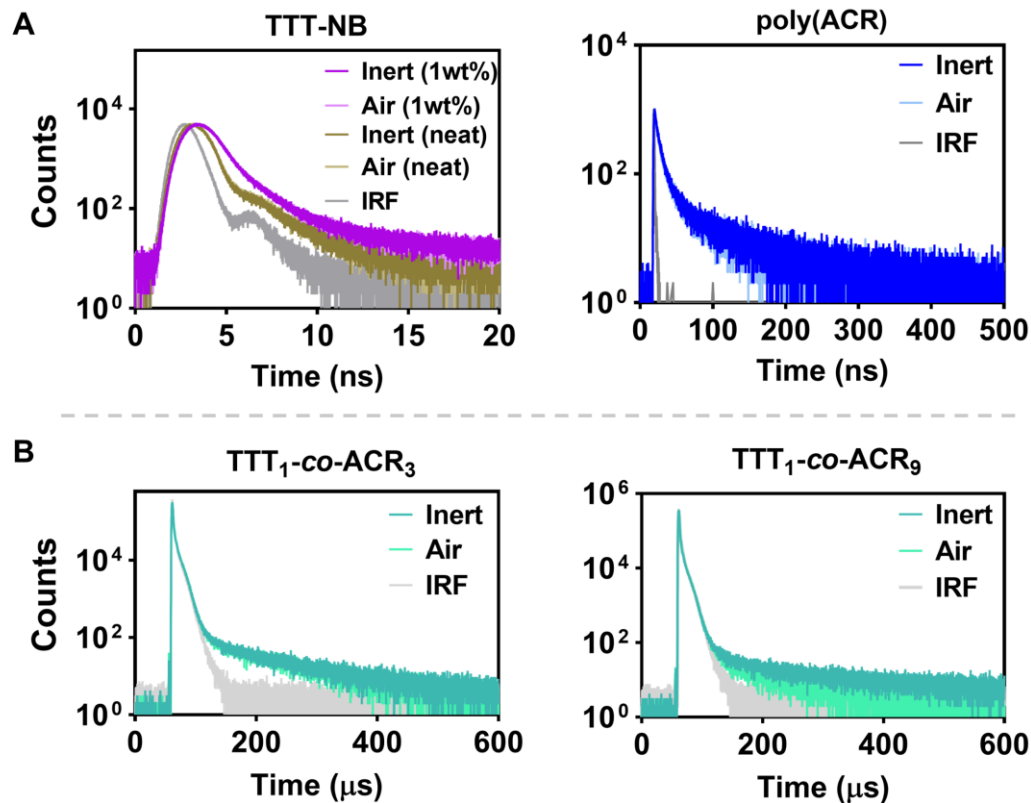


**Figure S19.** (A) PL decays of TTT-NB in both neat film and 1 wt% doped PMMA, and neat film of poly(ACR) under air vs. inert conditions (measured using TCSPC, ex = 313 nm). (B) PL decays of neat copolymers films under air vs inert conditions.

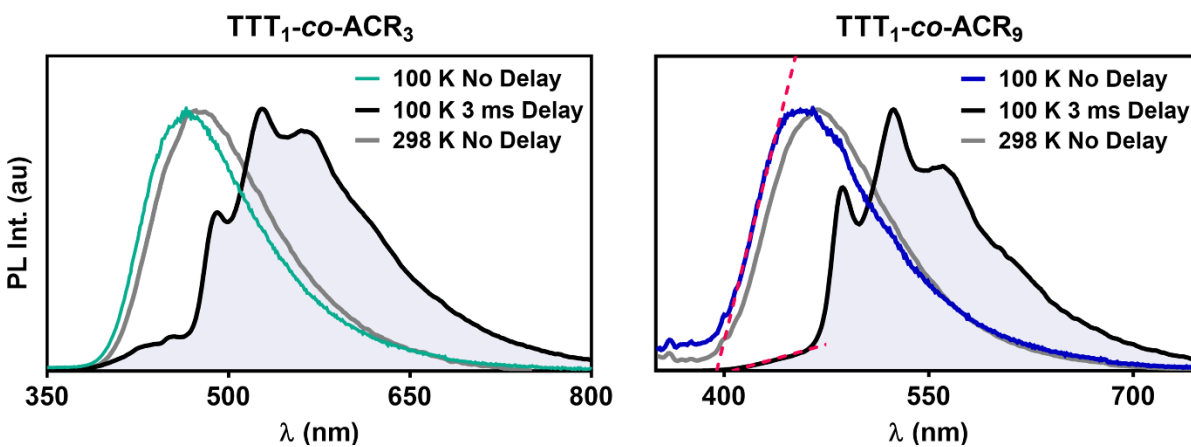


**Figure S20.** Steady state emission spectra of copolymers in neat films at 298 K or 77 K, and time-gated emission spectra at 77 K (emission onsets fitted in dashed red line, ex = 290 nm).

## 6. Cyclic Voltammetry and Tauc plot

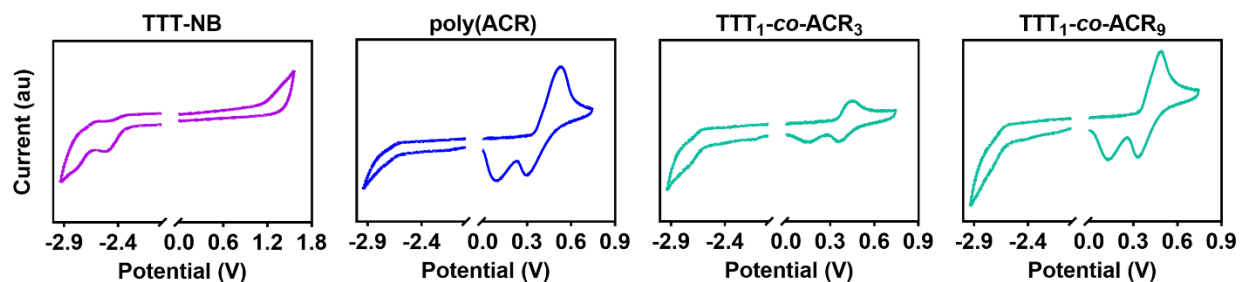


**Figure S21.** Cyclic voltammograms measured at  $2 \text{ mg mL}^{-1}$  in degassed 1,2-difluorobenzene relative to  $\text{Fc}^{0/+}$ , with  $0.02 \text{ M}$  tetrabutylammonium hexafluorophosphate (1<sup>st</sup> cycle is shown).

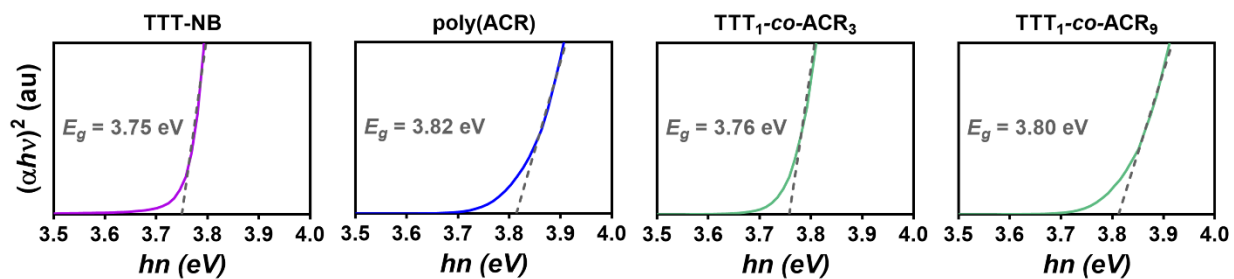


**Figure S22.** Tauc plot at concentrations of  $0.01 \text{ mg mL}^{-1}$  in toluene, with their  $E_{\text{opt}}$  values displayed from their respective onset energies (in eV).

## 7. Theoretical Calculations

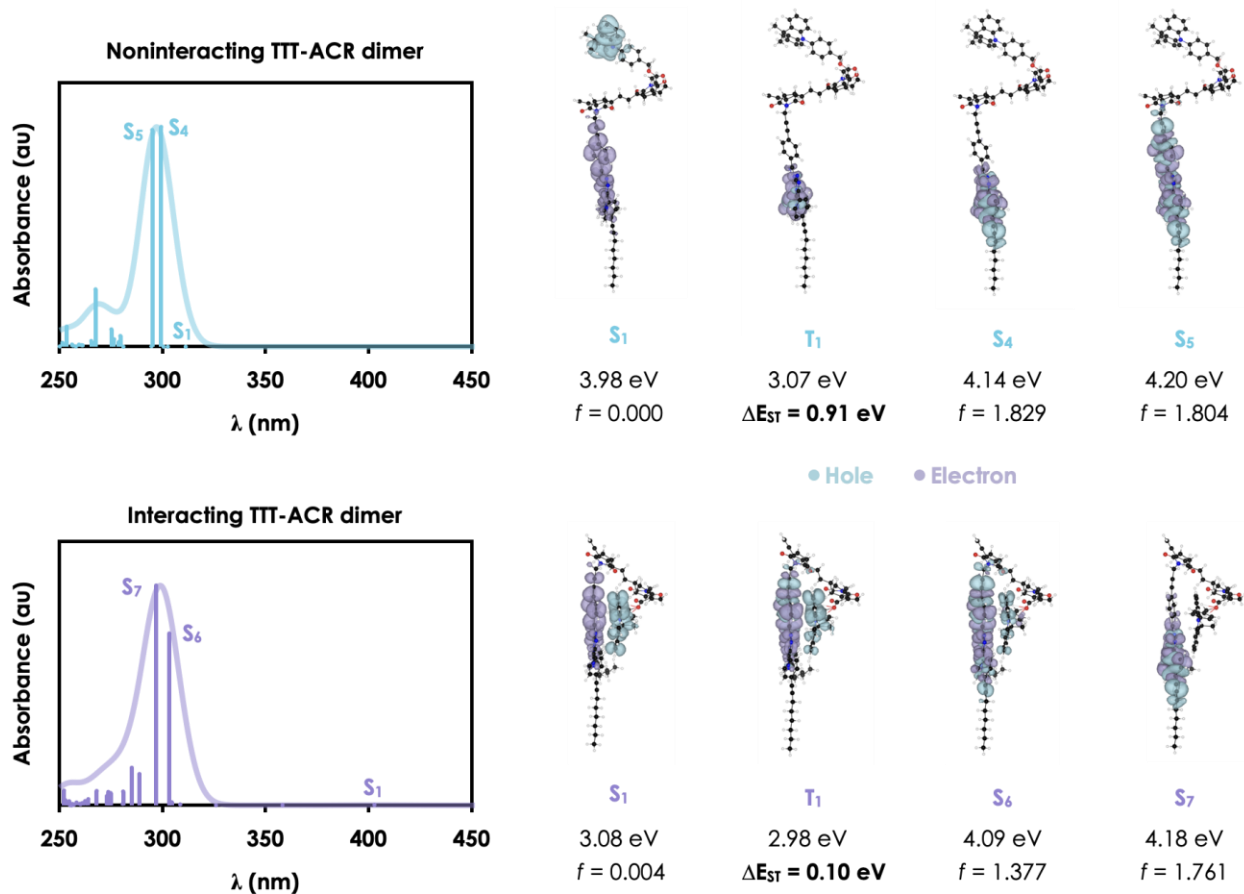


**Figure S23.** Calculated UV-vis absorbance spectra for the noninteracting and interacting TTT-ACR dimers, with vertical excitations contributing to the calculated spectra shown as bars. Hole-electron analysis is shown for relevant excited states with corresponding energies and oscillator strengths.

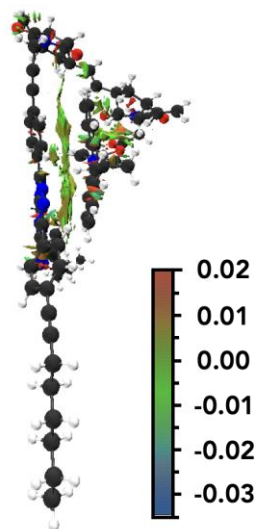


**Figure S24.** Isosurface of the reduced density gradient for the interacting TTT-ACR dimer (isovalue: 0.63) to visualize the van der Waals interactions between the donor and acceptor moieties. Red indicates repulsive interactions such as steric interactions, green indicates weak interactions such as van der Waals interactions, and blue indicates attractive interactions such as hydrogen bonding.

## 8. Optimized structures of ground-state geometries

### Non-interacting dimer

EE: -4507.004876 Hartree

EE + Thermal Free Energy Correction: -4505.610715 Hartree

Atom	x (Å)	y (Å)	z (Å)	Atom	x (Å)	y (Å)	z (Å)
C	-4.283	-0.897	-5.49	C	-13.397	1.8	2.688
C	-4.189	-0.671	-4.181	O	-9.985	1.258	6.437
C	-3.746	-1.671	-3.15	C	-7.052	-3.322	5.319
C	-3.866	-3.158	-3.559	O	-7.728	-3.723	6.226
C	-2.611	-3.715	-4.205	O	-6.594	-1.119	2.671
N	-2.049	-4.628	-3.316	C	-5.708	-3.853	4.848
C	-0.76	-5.25	-3.547	C	-5.773	-5.343	4.407
C	0.354	-4.375	-3.161	C	-4.966	-5.342	3.1
C	1.264	-3.637	-2.852	C	-4.532	-1.624	-1.832
C	2.338	-2.751	-2.497	H	-4.605	-0.108	-6.172
C	2.463	-1.504	-3.132	H	-4.006	-1.86	-5.927
C	3.5	-0.649	-2.792	H	-4.426	0.324	-3.789
C	3.272	-3.116	-1.516	H	-2.687	-1.466	-2.905
C	4.314	-2.262	-1.177	H	-4.716	-3.29	-4.244
C	4.441	-1.025	-1.819	H	-0.688	-5.492	-4.617
C	5.468	-0.026	-1.481	H	-0.735	-6.178	-2.959
N	5.26	1.262	-1.56	H	1.739	-1.218	-3.894
N	6.39	1.934	-1.225	H	3.599	0.325	-3.272
C	7.281	1.047	-0.935	H	3.173	-4.08	-1.016



C	-14.848	0.596	-2.839	H	-5.15	-6.23	2.479
C	-14.355	1.71	-3.754	H	-3.887	-5.312	3.33
C	-12.902	1.371	-4.162	H	-4.35	-0.709	-1.251
C	-15.197	1.836	-5.023	H	-5.613	-1.678	-2.048
C	-14.317	3.006	-2.951	H	-3.061	-2.732	-0.718
C	-13.854	2.945	-1.62	C	-5.281	-6.298	5.452
C	-13.609	4.131	-0.913	H	-4.22	-6.205	5.718
C	-13.871	5.366	-1.5	C	-6.034	-7.21	6.062
C	-14.389	5.436	-2.789	H	-5.619	-7.875	6.822
C	-14.601	4.256	-3.501	H	-7.096	-7.312	5.828
C	-13.933	1.865	1.407	H	-6.821	-5.593	4.172

## Interacting dimer

EE: -4507.053729 Hartree

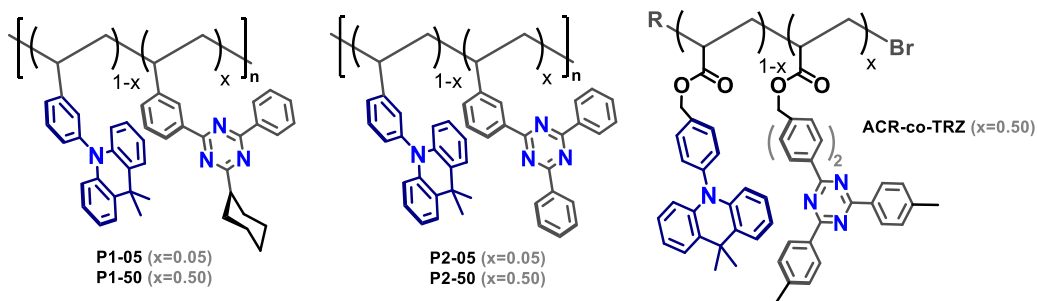
EE + Thermal Free Energy Correction: -4505.635393 Hartree

Atom	x (Å)	y (Å)	z (Å)	Atom	x (Å)	y (Å)	z (Å)
C	-10.834	-2.659	-5.069	C	-2.867	2.151	0.111
C	-10.151	-1.756	-4.367	O	-5.942	5.707	1.926
C	-9.01	-2.065	-3.438	C	-5.965	1.358	4.549
C	-9.035	-3.479	-2.801	O	-6.145	1.544	5.722
C	-8.134	-4.472	-3.515	O	-6.461	2.32	1.254
N	-7.172	-4.903	-2.604	C	-5.136	0.268	3.885
C	-6.041	-5.735	-2.97	C	-5.484	-1.172	4.357
C	-4.801	-4.949	-2.975	C	-5.855	-1.894	3.047
C	-3.82	-4.241	-2.92	C	-8.887	-1.136	-2.221
C	-2.679	-3.38	-2.792	H	-11.638	-2.358	-5.742
C	-2.744	-2.044	-3.222	H	-10.585	-3.723	-5.022
C	-1.665	-1.196	-3.029	H	-10.393	-0.693	-4.477
C	-1.509	-3.839	-2.178	H	-8.073	-1.966	-4.017
C	-0.434	-2.984	-1.96	H	-10.06	-3.876	-2.789
C	-0.499	-1.653	-2.385	H	-6.258	-6.146	-3.966
C	0.559	-0.644	-2.194	H	-5.956	-6.562	-2.251
N	0.315	0.633	-2.348	H	-3.647	-1.681	-3.713
N	1.452	1.351	-2.199	H	-1.706	-0.164	-3.375
C	2.392	0.506	-1.944	H	-1.454	-4.872	-1.835
N	1.924	-0.792	-1.923	H	0.452	-3.363	-1.458
C	2.774	-1.854	-1.619	H	5.342	-4.598	0.709
N	2.516	-3.097	-1.386	H	7.637	-5.317	1.371
N	3.684	-3.697	-1.049	H	12.752	-5.943	0.405
C	4.651	-2.819	-1.079	H	12.405	-5.555	2.09
C	6.039	-3.139	-0.714	H	13.429	-3.554	-0.007
C	6.221	-4.14	0.253	H	13.086	-3.166	1.679
C	7.497	-4.544	0.614	H	15.164	-5.222	0.728
C	8.624	-3.962	0.01	H	14.821	-4.838	2.414
C	9.948	-4.376	0.384	H	15.862	-2.84	0.328
C	11.063	-4.732	0.7	H	15.522	-2.458	2.015
C	12.422	-5.13	1.073	H	17.587	-4.514	1.055
C	13.427	-3.974	1.011	H	17.247	-4.134	2.741
C	14.836	-4.408	1.397	H	18.322	-2.128	0.659
C	15.85	-3.271	1.344	H	17.98	-1.746	2.358
C	17.264	-3.701	1.727	H	19.278	-2.889	1.949
C	18.269	-2.556	1.671	H	9.306	-2.524	-1.446
C	8.435	-2.973	-0.968	H	7.037	-1.793	-2.087
C	7.158	-2.565	-1.33	H	6.063	3.757	-2.591
N	4.12	-1.593	-1.468	H	5.595	6.201	-2.749
C	4.622	-0.297	-1.491	H	1.963	10.303	-1.506
N	5.826	0.134	-1.313	H	2.602	10.337	-3.151
N	5.771	1.489	-1.382	H	4.94	10.609	-2.206

C	4.54	1.872	-1.602	H	4.252	10.693	-0.584
C	4.15	3.286	-1.723	H	4.749	12.949	-1.527
C	5.11	4.162	-2.25	H	3.674	12.647	-2.889
C	4.851	5.522	-2.331	H	2.767	12.693	0.044
C	3.628	6.042	-1.875	H	1.709	12.548	-1.36
C	3.354	7.449	-1.959	H	2.467	14.8	-2.166
C	3.115	8.636	-2.032	H	3.495	14.957	-0.745
C	2.855	10.074	-2.11	H	0.425	14.664	-0.684
C	4.047	10.921	-1.643	H	1.326	16.168	-0.395
C	3.826	12.422	-1.819	H	1.46	14.816	0.75
C	2.659	12.989	-1.015	H	1.731	5.559	-0.969
C	2.554	14.509	-1.106	H	2.178	3.136	-0.838
C	1.378	15.073	-0.317	H	-9.139	-3.534	-0.581
C	2.678	5.162	-1.332	H	-8.715	-1.213	0.642
C	2.934	3.798	-1.255	H	-5.682	-1.376	0.167
N	3.74	0.735	-1.697	H	-7.454	-0.531	2.559
C	-7.29	-4.332	-1.34	H	-4.628	0.325	1.722
O	-6.556	-4.575	-0.42	H	-7.868	3.16	4.72
O	-8.195	-4.829	-4.66	H	-7.958	3.498	2.958
C	-8.428	-3.336	-1.395	H	-7.046	5.447	4.248
C	-7.904	-1.876	-1.309	H	-5.713	4.408	4.85
C	-7.777	-1.381	0.096	H	-4.672	4.069	0.594
C	-6.613	-1.193	0.719	H	-3.278	4.95	1.27
C	-6.463	-0.803	2.153	H	-2.755	2.72	3.459
C	-5.494	0.38	2.399	H	-1.44	0.593	3.358
C	-6.183	1.719	2.259	H	-3.365	-1.214	0.38
N	-6.514	2.147	3.542	H	-4.489	-3.42	0.142
C	-7.282	3.344	3.81	H	-3.243	-5.499	0.651
C	-6.405	4.589	4.016	H	-0.905	-5.371	1.439
C	-5.633	4.904	2.758	H	-0.188	-3.858	3.943
O	-4.559	4.102	2.653	H	-0.268	-2.085	3.766
C	-3.912	4.056	1.388	H	1.301	-2.869	4.092
C	-3.099	2.789	1.334	H	0.938	-5.273	2.155
C	-2.573	2.229	2.502	H	2.389	-4.31	2.346
C	-1.848	1.041	2.45	H	1.678	-4.494	0.721
C	-1.623	0.407	1.226	H	0.588	1.419	0.865
N	-0.856	-0.798	1.206	H	3.045	1.602	1.044
C	-1.492	-2.044	1.066	H	4.424	-0.44	1.482
C	-2.823	-2.126	0.625	H	3.304	-2.608	1.833
C	-3.452	-3.36	0.484	H	-1.918	0.491	-0.905
C	-2.755	-4.53	0.768	H	-3.279	2.575	-0.807
C	-1.434	-4.448	1.204	H	-4.08	0.507	4.078
C	-0.782	-3.224	1.374	H	-6.532	-2.746	3.197
C	0.59	-3.124	2.038	H	-4.94	-2.277	2.565
C	0.345	-2.976	3.559	H	-8.547	-0.124	-2.483
C	1.445	-4.371	1.789	H	-9.865	-1.047	-1.718
C	1.303	-1.854	1.58	H	-6.906	-1.847	-1.783
C	0.538	-0.705	1.285	C	-4.36	-1.833	5.099
C	1.181	0.531	1.084	H	-3.449	-2.007	4.51
C	2.566	0.629	1.174	C	-4.401	-2.203	6.377
C	3.336	-0.507	1.42	H	-3.546	-2.678	6.86
C	2.695	-1.73	1.616	H	-5.295	-2.034	6.983
C	-2.12	0.976	0.051	H	-6.362	-1.123	5.021



## 9. Comparison to previously reported triazine based TSCT-TADF polymers



**Scheme S1.** Previously reported triazine based TSCT-TADF polymers.

**Table S1:** Photophysical comparison of TTT copolymers with previously reported triazine copolymers.

Entry	$\lambda_{\text{absmax}}$ (nm)	$\lambda_{\text{em}}^{\text{Inert}}$ (nm)	$\Phi^{\text{air}}/\Phi^{\text{N2}}$	$\tau_{\text{d}}^{\text{Inert}}$ ( $\mu\text{s}$ )	$\Phi^{\text{air}}_{\text{film}}/\Phi^{\text{N2}}_{\text{film}}$
TTT <sub>1-co-ACR</sub> <sub>3</sub>	290	349, 530	0.05/0.09	0.83	0.01/--
TTT <sub>1-co-ACR</sub> <sub>9</sub>	289	348, 527	0.01/0.06	1.3	0.04/--
<b>P1-05</b> <sup>a</sup>	350	469	--	0.36	--/0.29
<b>P1-50</b> <sup>a</sup>	250	477	--	0.21	--/0.32
<b>P2-05</b> <sup>a</sup>	375	486	--	1.28	--/0.51
<b>P2-50</b> <sup>a</sup>	375	489	--	1.17	--/0.60
<b>ACR-co-TRZ</b>	289	346, 507	0.24/0.62	--	0.25/--

\*All measurements collected in toluene ( $0.01 \text{ mg mL}^{-1}$ ) unless otherwise noted; Data for **P1**, **P2** and **ACR-co-TRZ** are based on previous reports<sup>16,17</sup>; <sup>a</sup> Concentration was  $0.001 \text{ mg mL}^{-1}$ .

## 10. NMR tracking of the copolymerization

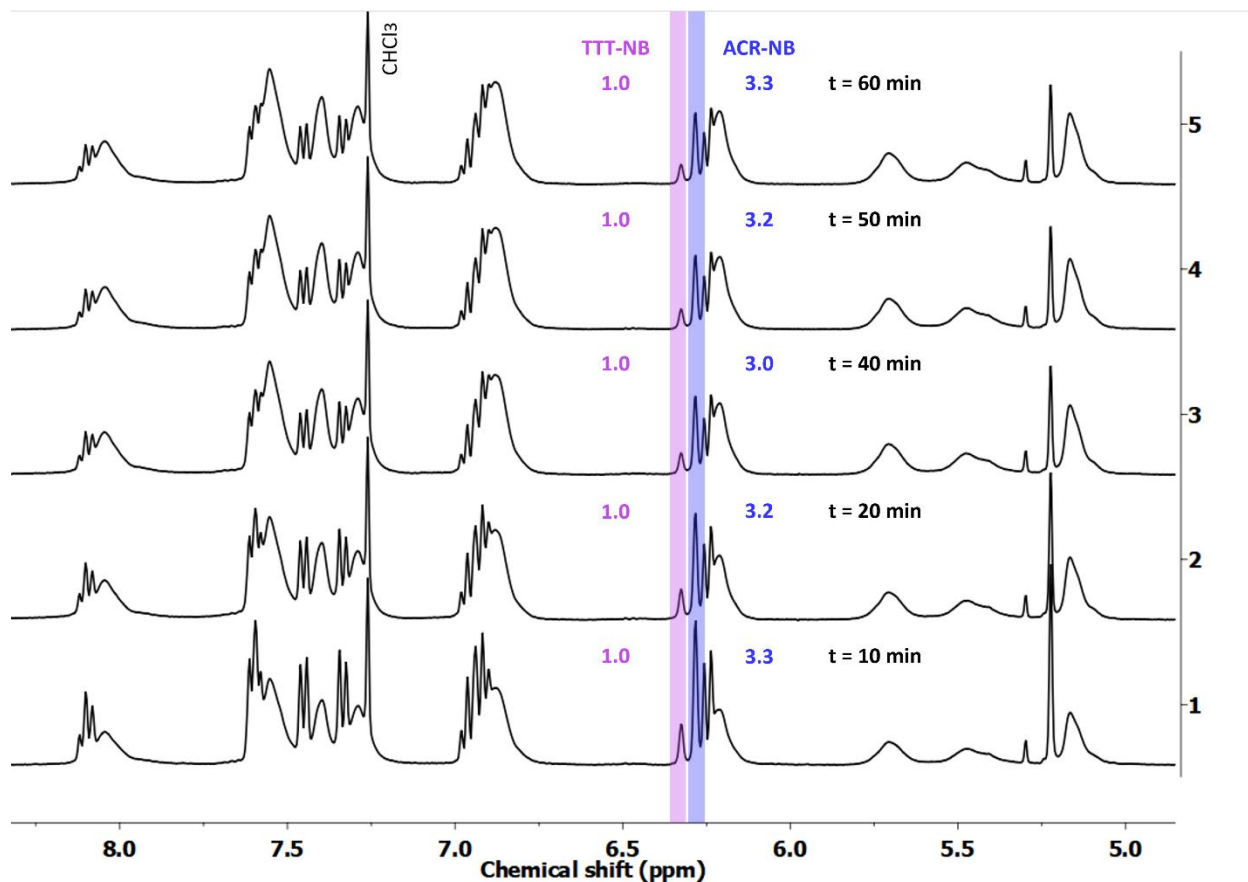


**Figure S25.** <sup>1</sup>H-NMR spectrum (CDCl<sub>3</sub>, 400 MHz) taken at different time intervals during the polymerization of **TTT<sub>1</sub>-co-ACR<sub>3</sub>** in a sealed NMR tube. The coloured numbers indicate the relative integration of norbornene signals from unreacted **TTT-NB** and **ACR-NB** in the mixture.

## 10. References

- 1 M. S. Sanford, J. A. Love and R. H. Grubbs, *Organometallics*, 2001, **20**, 5314–5318.
- 2 M. J. Frisch, G. W. Trucks, H. B. Schlegel, G. E. Scuseria, M. A. Robb, J. R. Cheeseman, G. Scalmani, V. Barone, G. A. Petersson, H. Nakatsuji, X. Li, M. Caricato, A. V. Marenich, J. Bloino, J. B.G., R. Gomperts, B. Mennucci, H. P. Hratchian, J. V. Ortiz, A. F. Izmaylov, J. L. Sonnenberg, D. Williams-Young, F. Ding, F. Lipparini, F. Egidi, J. Goings, B. Peng, A. Petrone, T. Henderson, D. Ranasinghe, V. G. Zakrzewski, J. Gao, N. Rega, G. Zheng, W. Liang, M. Hada, M. Ehara, K. Toyota, R. Fukuda, J. Hasegawa, M. Ishida, T. Nakajima, Y. Honda, O. Kitao, H. Nakai, T. Vreven, K. Throssell, M. J. J.A., J. E. Peralta, F. Ogliaro, M. J. Bearpark, J. J. Heyd, E. N. Brothers, K. N. Kudin, V. N. Staroverov, T. A. Keith, R. Kobayashi, J. Normand, A. P. Raghavachari, K. Rendell, J. C. Burant, S. S. Iyengar, J. Tomasi, M. Cossi, J. M. Millam, M. Klene, C. Adamo, R. Cammi, J. W. Ochterski, R. L. Martin, K. Morokuma, O. Farkas, J. B. Foresman and D. J. Fox, *Gaussian 16, Gaussian, Inc. Wallingford, CT*, 2016.
- 3 Y. Zhao and D. G. Truhlar, *Theor. Chem. Acc.*, 2008, **120**, 215–241.
- 4 F. Weigend and R. Ahlrichs, *Phys. Chem. Chem. Phys.*, 2005, **7**, 3297–3305.
- 5 S. Bhandari, M. S. Cheung, E. Geva, L. Kronik and B. D. Dunietz, *J. Chem. Theory Comput.*, 2018, **14**, 6287–6294.
- 6 T. M. Henderson, A. F. Izmaylov, G. Scalmani and G. E. Scuseria, *J. Chem. Phys.*, 2009, **131**, 44108.
- 7 J. P. Perdew, K. Burke and M. Ernzerhof, *Phys. Rev. Lett.*, 1996, **77**, 3865–3868.
- 8 T. Stein, L. Kronik and R. Baer, *J. Am. Chem. Soc.*, 2009, **131**, 2818–2820.
- 9 F. Neese, *WIREs Comput. Mol. Sci.*, 2012, **2**, 73–78.
- 10 F. Neese, *WIREs Comput. Mol. Sci.*, 2022, **12**, e1606.
- 11 T. Lu and F. Chen, *J. Comput. Chem.*, 2012, **33**, 580–592.
- 12 E. R. Johnson, S. Keinan, P. Mori-Sánchez, J. Contreras-García, A. J. Cohen and W. Yang, *J. Am. Chem. Soc.*, 2010, **132**, 6498–6506.
- 13 Z. Liu, T. Lu and Q. Chen, *Carbon*, 2020, **165**, 461–467.
- 14 W. Humphrey, A. Dalke and K. Schulten, *J. Mol. Graph.*, 1996, **14**, 33–38.
- 15 K. Momma and F. Izumi, *J. Appl. Crystallogr.*, 2011, **44**, 1272–1276.
- 16 J. Hu, Q. Li, X. Wang, S. Shao, L. Wang, X. Jing and F. Wang, *Angew. Chem. Int. Ed.*, 2019, **58**, 8405–8409.
- 17 J. Poisson, C. M. Tonge, N. R. Paisley, E. R. Sauv e, H. McMillan, S. V Halldorson and Z. M. Hudson, *Macromolecules*, 2021, **54**, 2466–2476.